Article:
Moroz, Olga V., Jensen, Pernille F., McDonald, Sean P. et al. (17 more authors) (2018) Structural dynamics and catalytic properties of a multimodular xanthanase. ACS Catalysis. 6021–6034. ISSN 2155-5435

https://doi.org/10.1021/acscatal.8b00666

Supporting Information

Structural Dynamics and Catalytic Properties of a Multi-Modular Xanthanase

Olga V. Moroz[1,=], Pernille F. Jensen[2,=], Sean P. McDonald[3,=], Nicholas McGregor[4], Elena Blagova[1], Gerard Comamala[2], Dorotea R. Segura[5], Lars Anderson[5], Santhosh M. Vasu[5], Vasudeva P. Rao[5], Lars Giger[5], Trine Holst Sørensen[6], Rune Nygaard Monrad[5], Allan Svendsen[5], Jens E. Nielsen[5], Bernard Henrissat[7], Gideon J. Davies[1], Harry Brumer[3,4,], Kasper Rand[2,*] & Keith S. Wilson[1,*]*

1 York Structural Biology Laboratory, Department of Chemistry, the University of York, York YO10 5DD, UK

2 Department of Pharmacy, University of Copenhagen, Universitetsparken 2, 2100 Copenhagen, Denmark

3 Michael Smith Laboratories and Department of Biochemistry and Molecular Biology, University of British Columbia, Vancouver, British Columbia V6T 1Z4, Canada

4 Michael Smith Laboratories and Department of Chemistry, University of British Columbia, Vancouver, British Columbia V6T 1Z4, Canada

5 Novozymes A/S, Krogshojvej 36, DK-2880 Bagsvard, Denmark

6 Department of Science and Environment, INM, Roskilde University, 1 Universitetsvej, DK-4000, Roskilde Denmark

7 Architecture et Fonction des Macromolecules Biologiques, UMR 7857 CNRS, Aix-Marseille University, F-13288 Marseille, France; Institut National de la Recherche Agronomique, USC 1408 Architecture et Fonction des Macromolecules Biologiques, F-13288 Marseille, France; Department of Biological Sciences, King Abdulaziz University, Jeddah, Saudi Arabia

Corresponding Author

* Keith S. Wilson: keith.wilson@york.ac.uk

* Harry Brumer: brumer@msl.ubc.ca

* Kasper Rand: kasper.rand@sund.ku.dk

Author Contributions

=OVM, PFJ & SPM contributed equally. SPM performed enzymology, MS, and NMR experiments, analyzed the resulting data, and co-wrote the article. OVM and EB carried out the crystal screening and structure analysis. NM assisted with MS data acquisition and analysis. HB supervised research at UBC, analyzed data, and co-wrote the article. DRS, LA, SMV, VPR, THS and LG performed the experiments (cloning, expression, variant generation, purification, detergent stability and CBM binding); RNM, AS and JEN planned the experiments and co-wrote the article. PFJ planned and performed HDX-MS experiments, analyzed data and co-wrote the article. GK analyzed HDX-MS data and co-wrote the article. KDR planned HDX-MS experiments, analyzed data and supervised research at UCPH. KSW and GJD supervised the structural biology and co-wrote the article.

FIGURES

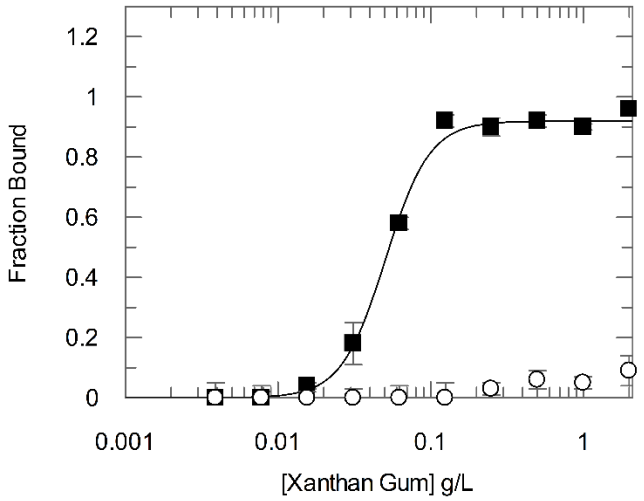

Figure S1 – The C terminal domain of PspXan9 defines a new family of xanthan-binding modules, termed CBM84. Fraction of Xanthan-bound protein (Protein-Xanthan) as function of xanthan gum concentration for the CBM84 domain (filled squares) with the purified GH12 endoglucanase EG3 from *Hypocrea jecorina* shown as a control (unfilled circles). Protein at 0.2 mg/ml was incubated with 0.004 – 2 mg/ml Xanthan gum (50 mM NaAcetate pH 5) and the fraction of bound *Hypocrea jecorina* EG3 (GH12) and CBM84 to Xanthan gum were estimated by measuring protein intrinsic fluorescence at λ_{EX} ~ 280 nm λ_{EM} ~ 303 nm (CBM84) and λ_{EX} ~ 280 nm λ_{EM} ~ 345 nm (*Hypocrea jecorina* EG3). Data for CBM84 were fit using a Hill equation to give K=0.05 g/L and a Hill coefficient of 2.9.

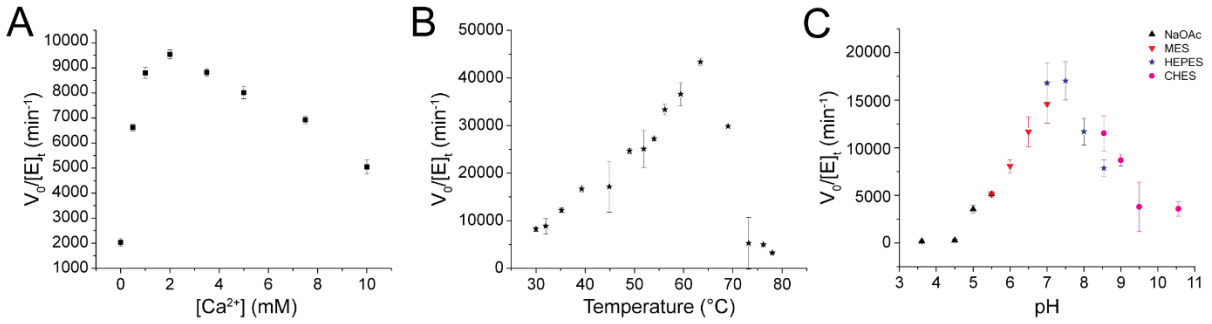

Figure S2 – Optimization of *Psp*Xan9 activity. *A*. The effect of calcium concentration on the hydrolytic activity of *Psp*Xan9 in 50 mM HEPES-NaOH buffer, pH 7.0. *B*. Temperature-rate profile for 10 min assays in the presence of 2 mM $CaCl_2$ Error bars represent the standard deviation over three replicates. *C*. pH-rate profile. For each, the rate of reducing-end formation with 0.5 mg·mL^{-1} of lyase-treated xanthan as the substrate was determined after a 10 min incubation.

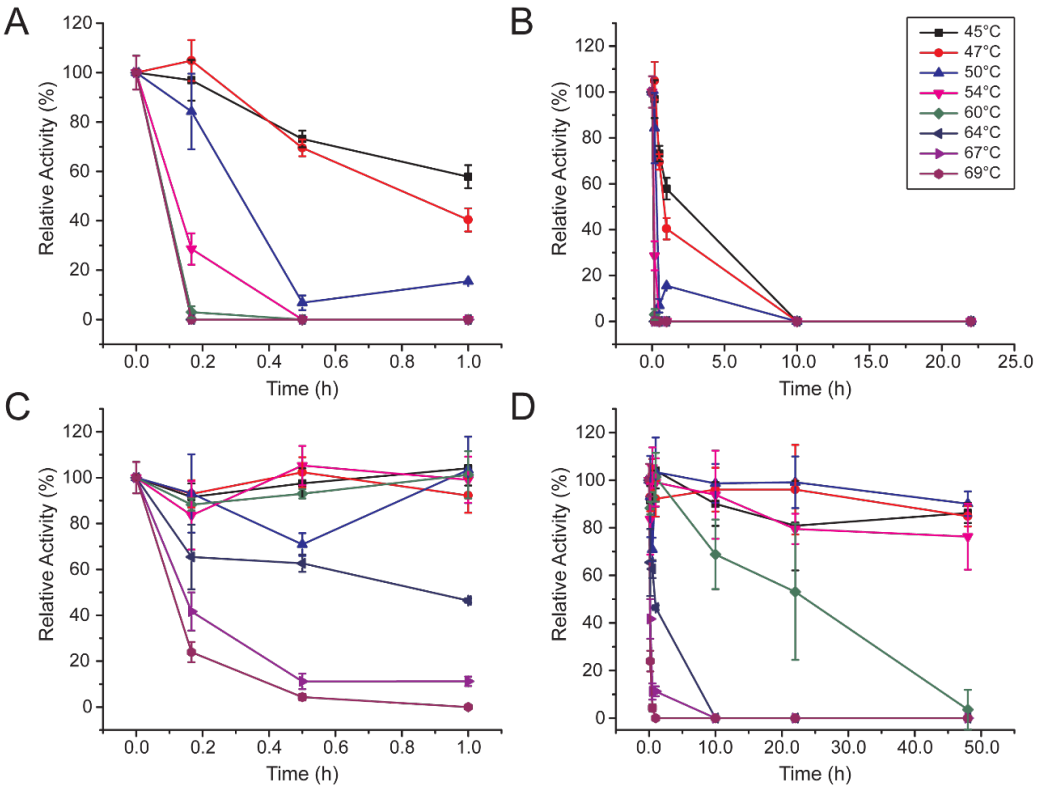

Figure S3 – The effect of Ca^{2+} ions on thermostability of *Psp*Xan9. *A*. Remaining activity of 16 nM *Psp*Xan9 following incubation at the indicated temperatures; *B*. shows an expansion of the data in panel A to cover a longer time period. *C*. remaining activity of 16 nM *Psp*Xan9 in the presence of 20 mM $CaCl_2$ following incubation at the indicated temperatures; *D*. shows an expansion of the data in panel *C* to cover a longer time period. After dilution, enzyme activity assays contained a final concentration of 2 mM $CaCl_2$ (*cf.* Fig. S003B). Error bars represent the standard deviation over three replicates.

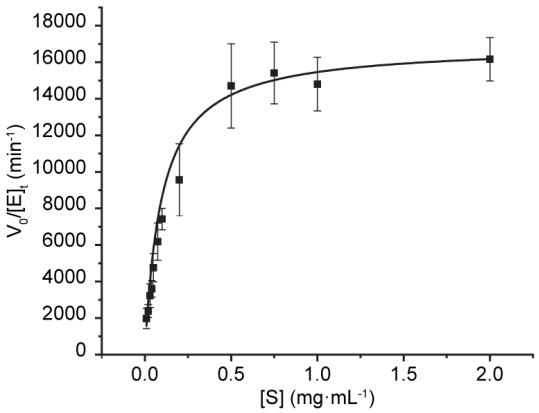

Figure S4 – Michaelis-Menten kinetics of *Psp*Xan9 activity on lyase-treated xanthan. *Psp*Xan9 kinetics were determined by quantifying activity after a 10 min incubation with lyase-treated xanthan concentrations between 0.01-2 mg·mL^{-1}. Error bars represent the standard deviation over three replicates.

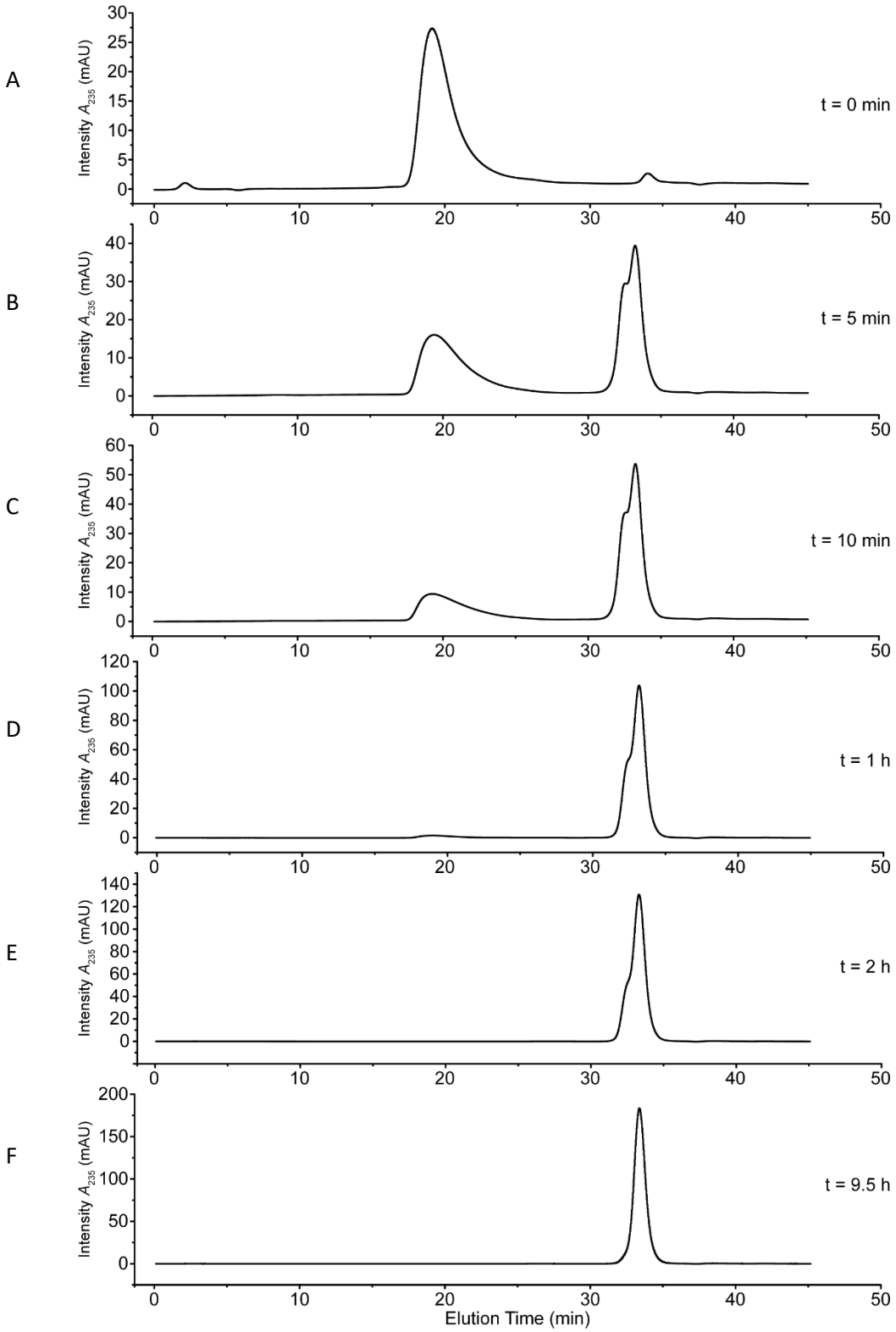

Figure S5 – HPLC-SEC-UV analysis of xanthan oligosaccharide products from a time course digestion with *Psp*Xan9. 2 mg·mL^{-1} of lyase-treated xanthan (*A*) was incubated with 16 nM *Psp*Xan9 at 55°C and sampled at various time points (*B-F*) for analysis by HPSEC.

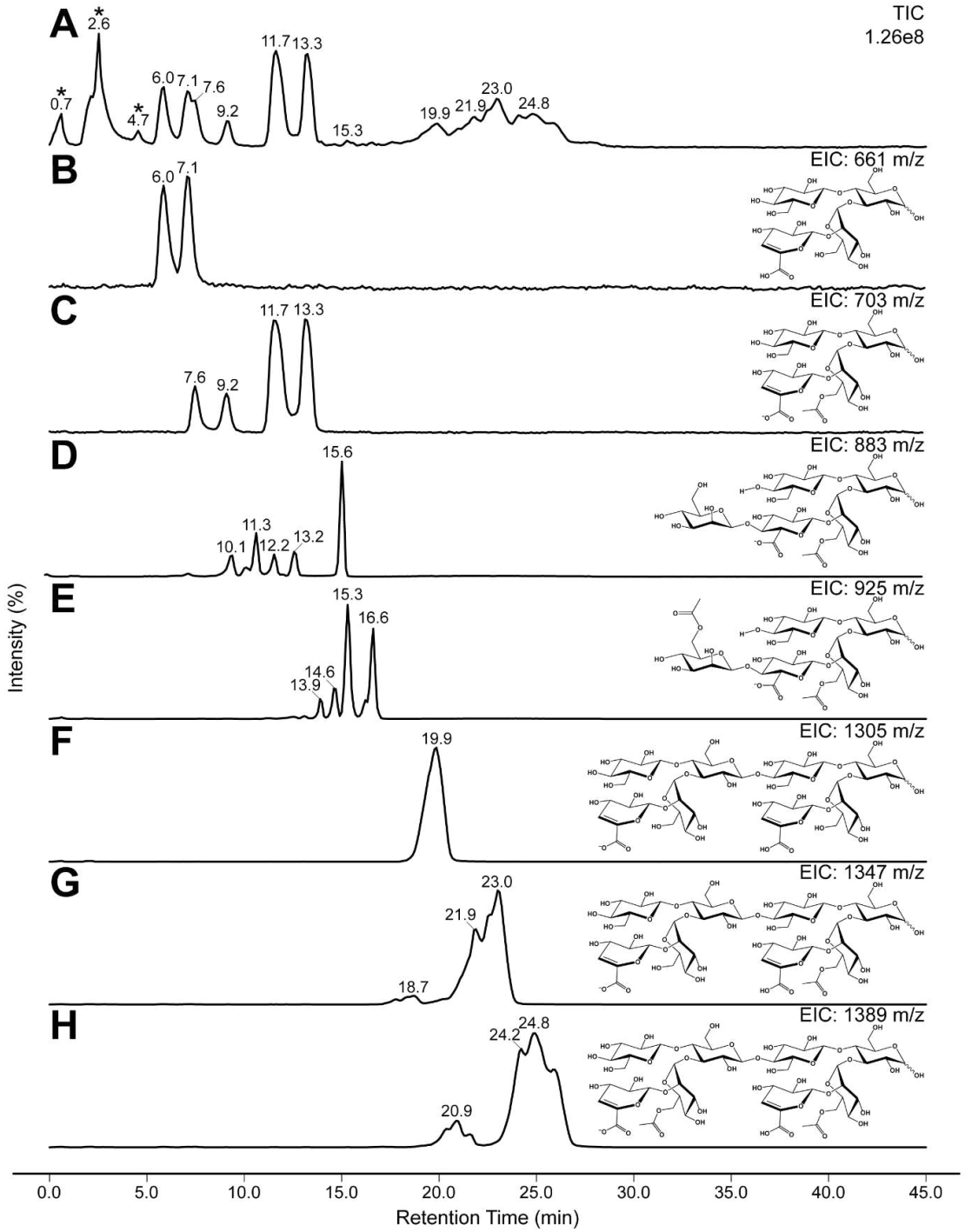

Figure S6 – LCMS chromatograms of partial digest products from *Psp*Xan9. Products from 2 h of degradation by 16 nM *Psp*Xan9 were separated over 45 min by liquid chromatography and analyzed using mass spectrometry with a scan range of 100 – 2000 m/z in negative-ion mode. The resulting total ion chromatogram (*A*) and extracted ion chromatograms (*B*-*H*) of expected products are displayed above, with corresponding structures and m/z values indicated on the right. Resolution of reducing-end anomers and acetylated variants is observed for some products. Non-carbohydrate peaks in the TIC are denoted with an asterisk symbol.

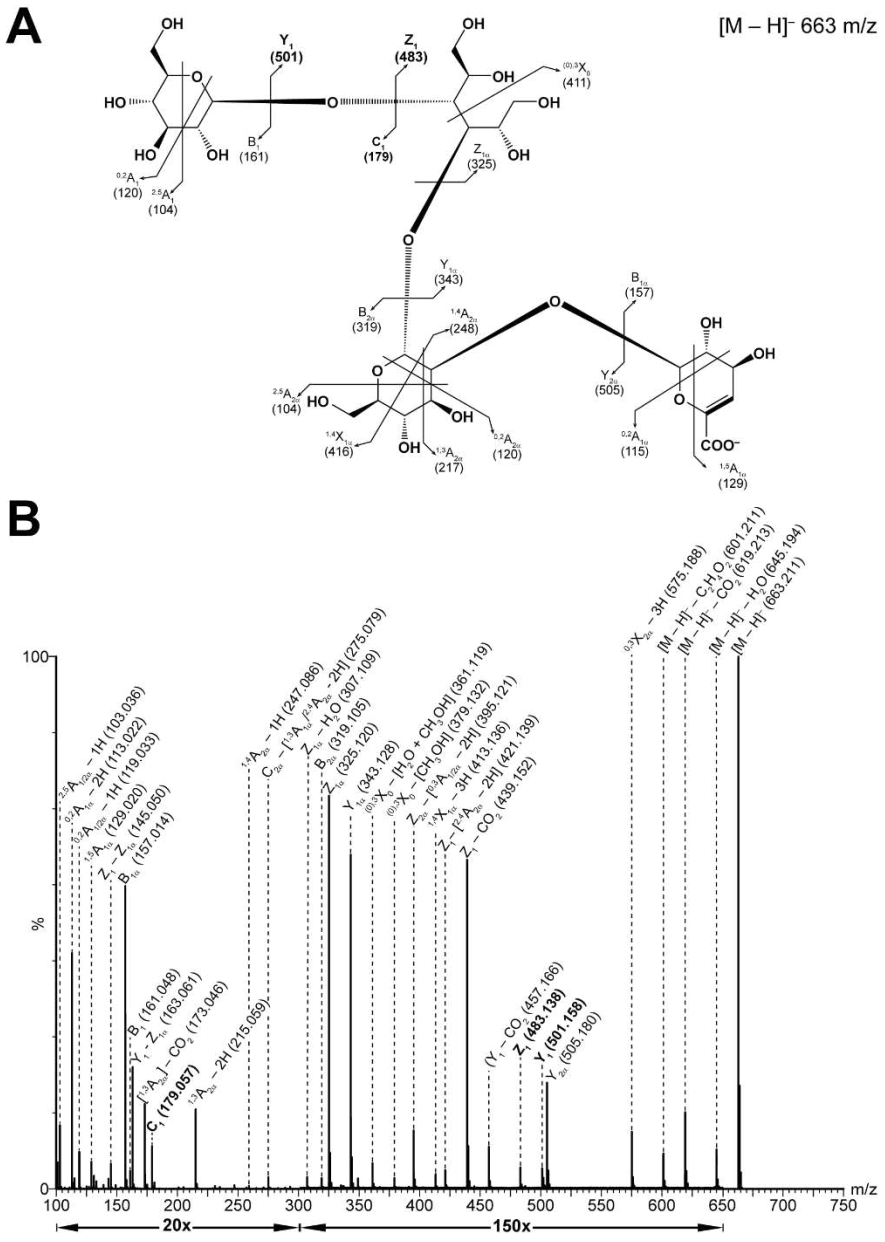

Figure S7 – MS/MS of the 663 m/z precursor ion, corresponding to the reduced, lyase-treated xanthan tetrasaccharide, from lyase-treated xanthan degradation by *Psp*Xan9. *A*. The fragmentation pattern of the 663 m/z precursor ion; *B*. The MSMS spectrum of the product ions from the fragmentation of 663 m/z. Selected regions are magnified and diagnostic peaks labelled in bold. Standard carbohydrate fragment nomenclature is used[1]. The presence of a forward slash in a peak label indicates the presence of alternative assignments. Regions within the bounds of arrows found below the x-axis, indicate the amount of magnification (if any) the region is being displayed at.

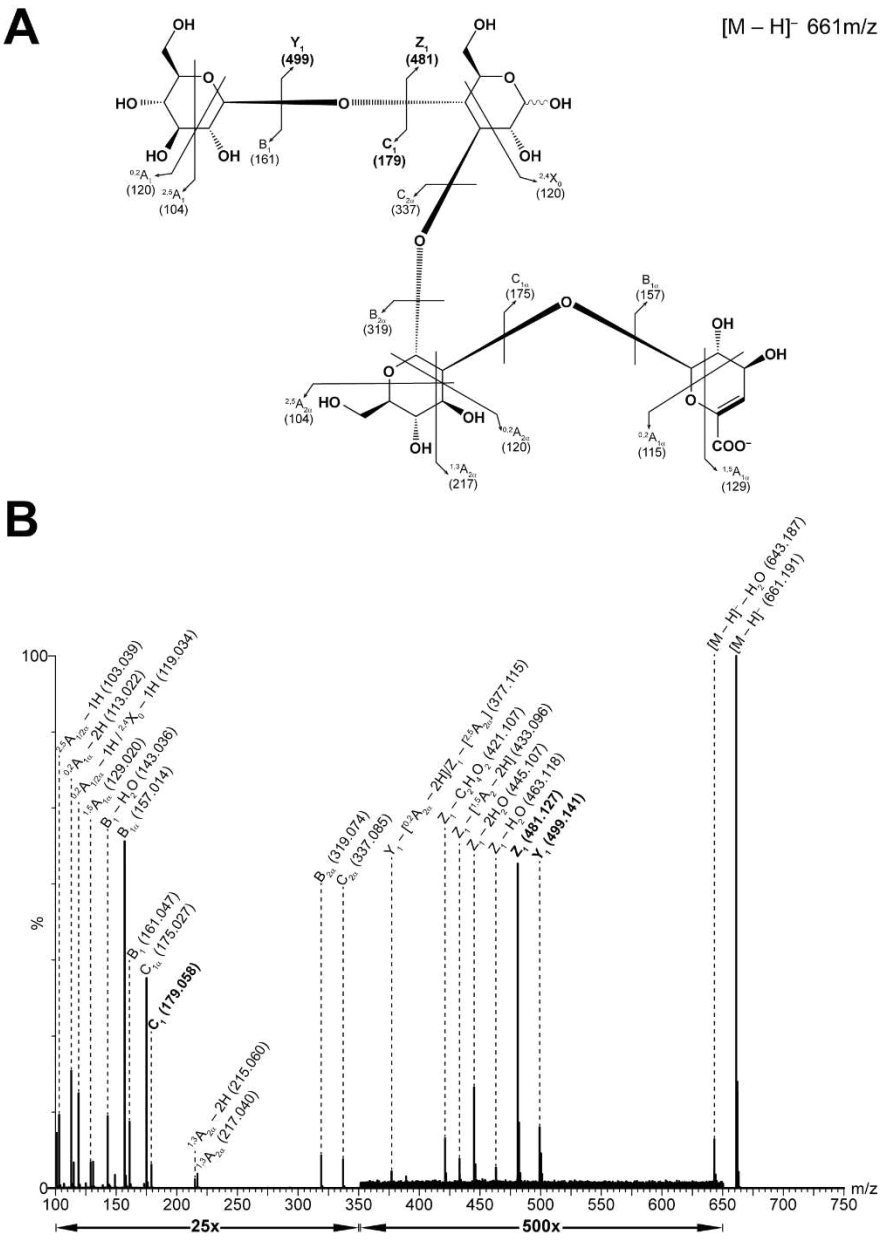

Figure S8 – MS/MS of the 661 m/z precursor ion, corresponding to the unacetylated, lyase-treated xanthan tetrasaccharide, from lyase-treated xanthan degradation by *Psp*Xan9. *A*. The fragmentation pattern of the 661 m/z precursor ion; *B*. The MSMS spectrum of the product ions from the fragmentation of 661 m/z. Selected regions are magnified and diagnostic peaks labelled in bold. Standard carbohydrate fragment nomenclature is used . The presence of a forward slash in a peak label indicates the presence of alternative assignments. Regions within the bounds of arrows found below the x-axis, indicate the amount of magnification (if any) the region is being displayed at.

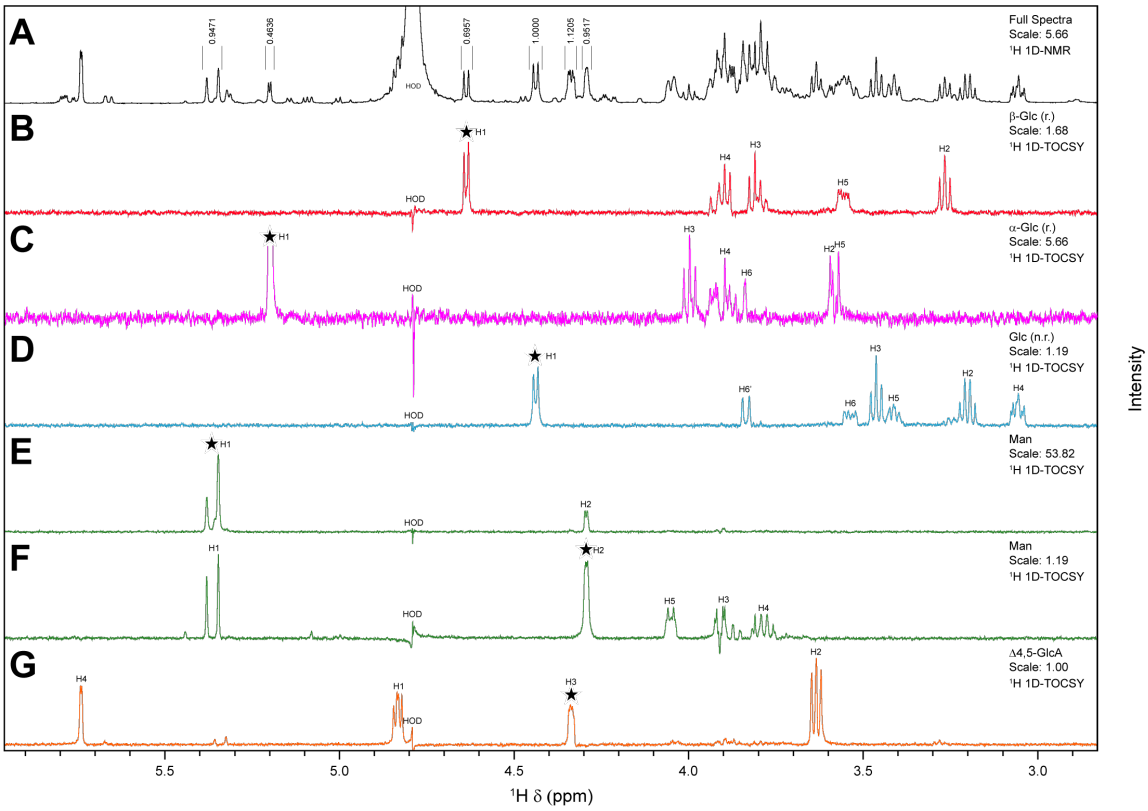

Figure S9 – Selective ^{1}H 1D-TOCSY experiment of deacetylated lyase-treated xanthan tetrasaccharides generated from lyase-treated xanthan degradation by *Psp*Xan9. *A*. Anomeric protons were targeted based on the full 1D-NMR spectrum, using the established anomeric proton region from between 4.3-5.5 ppm. Spectra corresponding to individual spin systems are displayed in various colors with: *B*. the reducing end (r.) β-glucose in red. *C*. the reducing end (r.) α-glucose in magenta. *D*. the nonreducing end (n.r.) β-glucose in light blue. *E*. α-mannose in green with irradiation on H1 at δ 5.36 ppm. *F*. α-mannose in green with irradiation on H2 at δ 4.29 ppm. *G*. β-Δ4,5-*ene*-glucuronic acid in orange. Proton integrations are presented on the full ^{1}H 1D-NMR spectrum above their corresponding peak. Irradiations from ^{1}H 1D-TOCSY experiments are displayed by black stars above corresponding peaks.

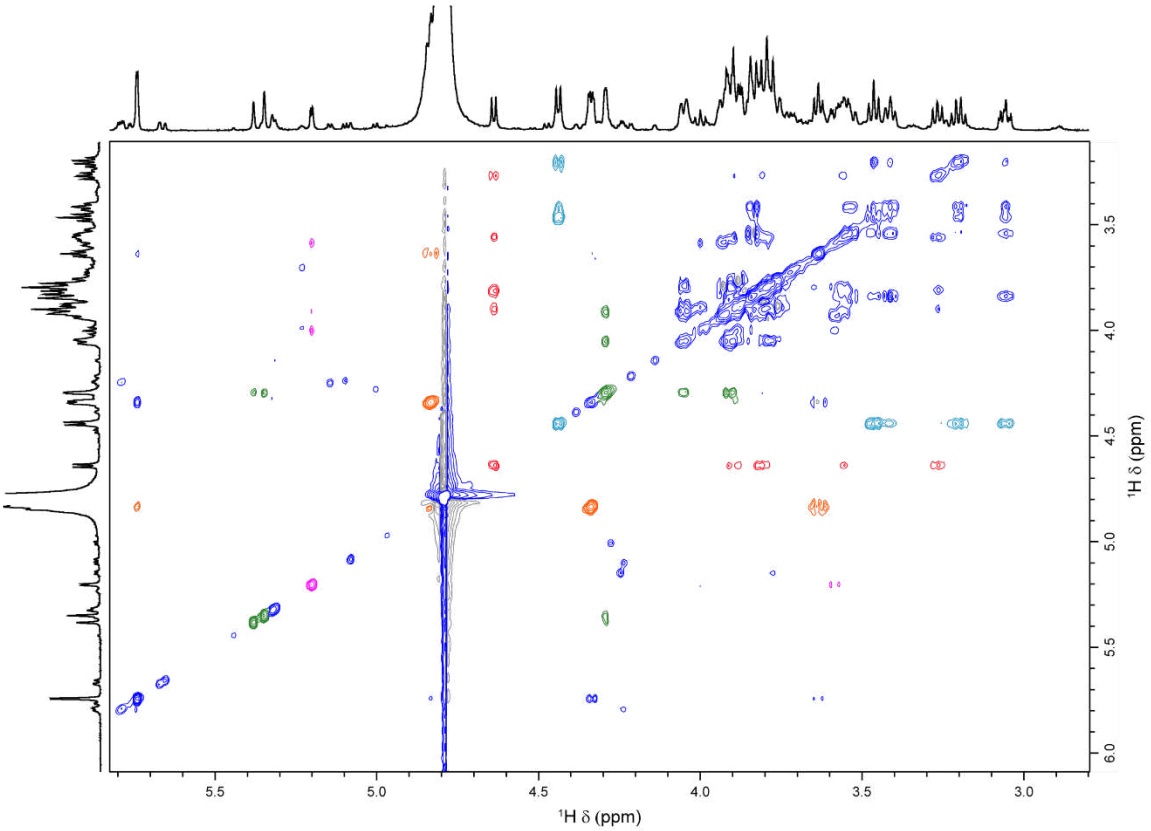

Figure S10 – ^{1}H 2D-TOCSY experiment of deacetylated lyase-treated xanthan tetrasaccharides generated from lyase-treated xanthan degradation by *Psp*Xan9. Each crosspeak indicates coupling between protons through magnetization transfer. Crosspeaks originating from the same spin system are shown in matching colours specific to each monosaccharide with the α/β reducing end glucose shown in magenta and red, respectively; the non-reducing end β-glucose shown in light blue; non-reducing α-mannose in green and β-Δ4,5-*ene*-glucuronic acid in orange. The remaining positive peaks are shown in dark blue and negative peaks are shown in grey. The crosspeaks that couple with the H2 diagonal peak of mannose are also shown in green due to the poor magnetization transfer from the anomeric proton.

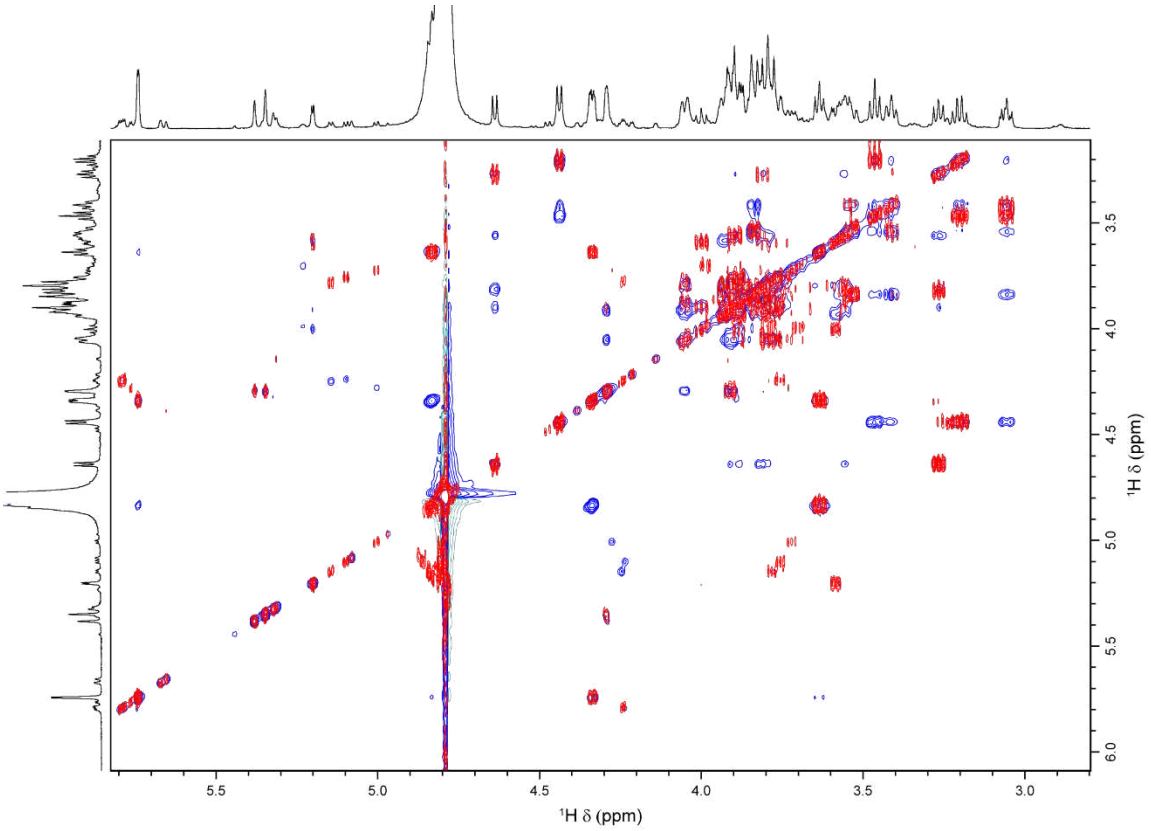

Figure S11 – ^{1}H 2D-TOCSY experiment overlaid with a ^{1}H 2D-COSY experiment of deacetylated lyase-treated xanthan tetrasaccharides generated from lyase-treated xanthan degradation by *Psp*Xan9. The ^{1}H 2D-TOCSY spectrum (see Figure S10 for more details) is overlaid with data from ^{1}H 2D-COSY allowing visualization of the crosspeaks that are ^{3}J-coupled to neighboring vicinal protons. Peaks from ^{1}H 2D-TOCSY are presented in dark blue, whereas ^{1}H 2D-COSY peaks are shown in red.

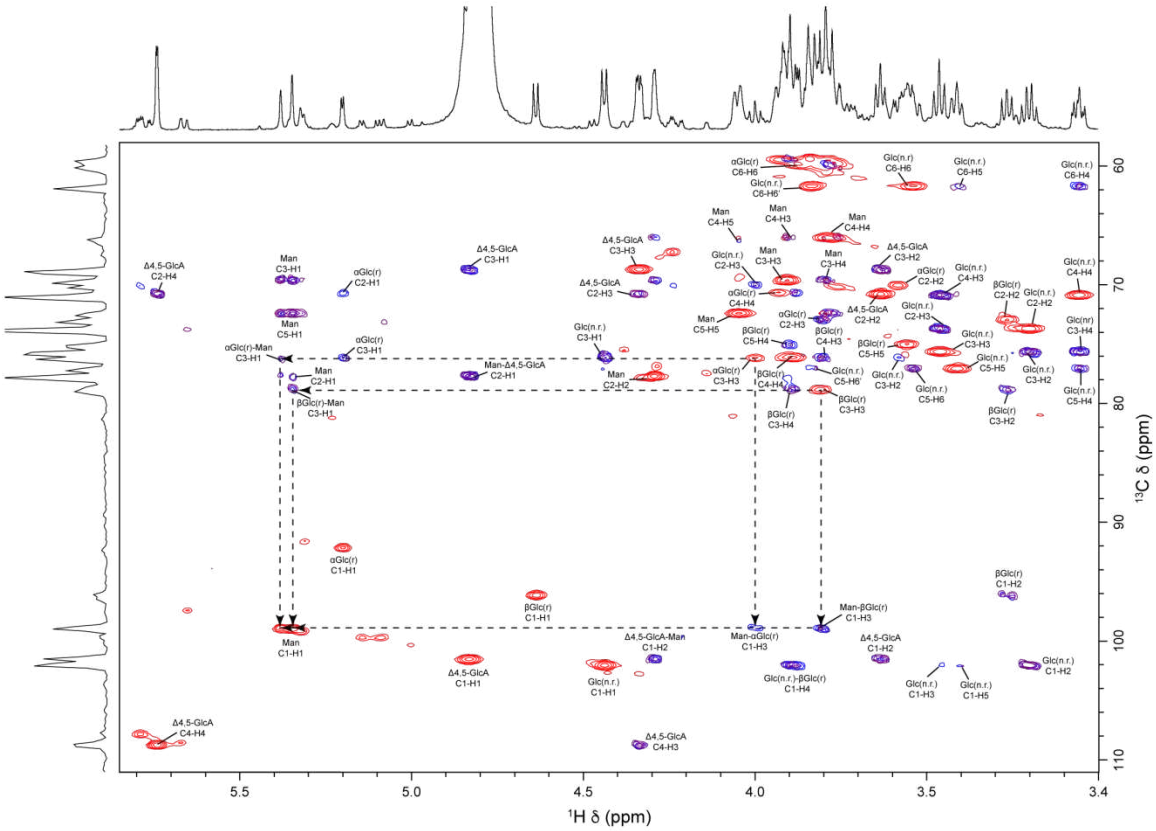

Figure S12 – Complete assignment of proton and carbon nuclei from deacetylated lyase-treated xanthan tetrasaccharides generated from lyase-treated xanthan degradation by *Psp*Xan9 using ^{1}H,^{13}C HSQC and ^{1}H,^{13}C HMBC experiments. Each red crosspeak corresponds to a $^{1}J_{C,H}$-coupling interaction from the HSQC experiment. $^{2}J_{C,H}$- or $^{3}J_{C,H}$-couplings were generated with HMBC experiments optimized for couplings at 5 Hz or 10 Hz, and are represented by blue and purple crosspeaks, respectively. The dotted arrows aid in tracing the path between the red HSQC crosspeaks of both of the C3-H3 peaks from the α/β-glucose reducing end (Glc(r.)) glucose through blue/purple HMBC crosspeaks to the red HSQC crosspeak of the C1-H1 of mannose. The notation states the sugar residue and its corresponding atom(s) below it. The sugar residue containing the carbon atom is always listed first, followed by the residue containing the proton atom. However, if both carbon and proton atoms exist within the same residue, the residue is only listed once. Abbreviations used: r., reducing end; n.r., nonreducing end; Glc, glucose; Man, mannose; Δ4,5-GlcA; Δ4,5-*ene*-glucuronic acid.

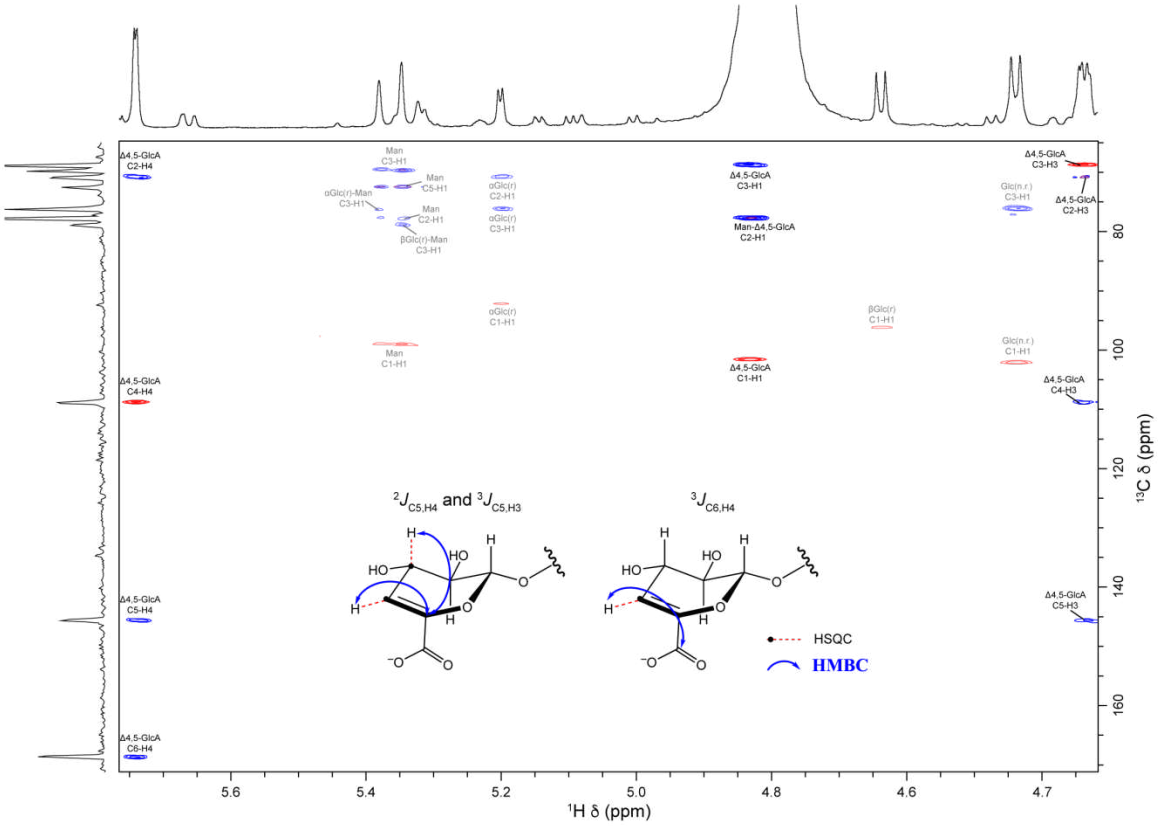

Figure S13 – Assignment of Δ4,5-*ene*-GlcA and a schematic illustrating the correlations for determination of C5 and C6 nuclei from deacetylated lyase-treated xanthan tetrasaccharides generated from lyase-treated xanthan degradation by *Psp*Xan9 using ^{1}H,^{13}C HSQC and ^{1}H,^{13}C HMBC experiments. Each red crosspeak corresponds to a $^1J_{C,H}$-coupling interaction from the HSQC experiment. $^2J_{C,H}$- or $^3J_{C,H}$-couplings were generated with HMBC experiments optimized for couplings at 5 Hz or 10 Hz, and are represented by blue and purple crosspeaks, respectively. The notation states the sugar residue and its corresponding atom(s) below it. The sugar residue containing the carbon atom is always listed first, followed by the residue containing the proton atom. However, if both carbon and proton atoms exist within the same residue, the residue is only listed once. Abbreviations used: r., reducing end; n.r., nonreducing end; Glc, glucose; Man, mannose; Δ4,5-GlcA; Δ4,5-*ene*-glucuronic acid.

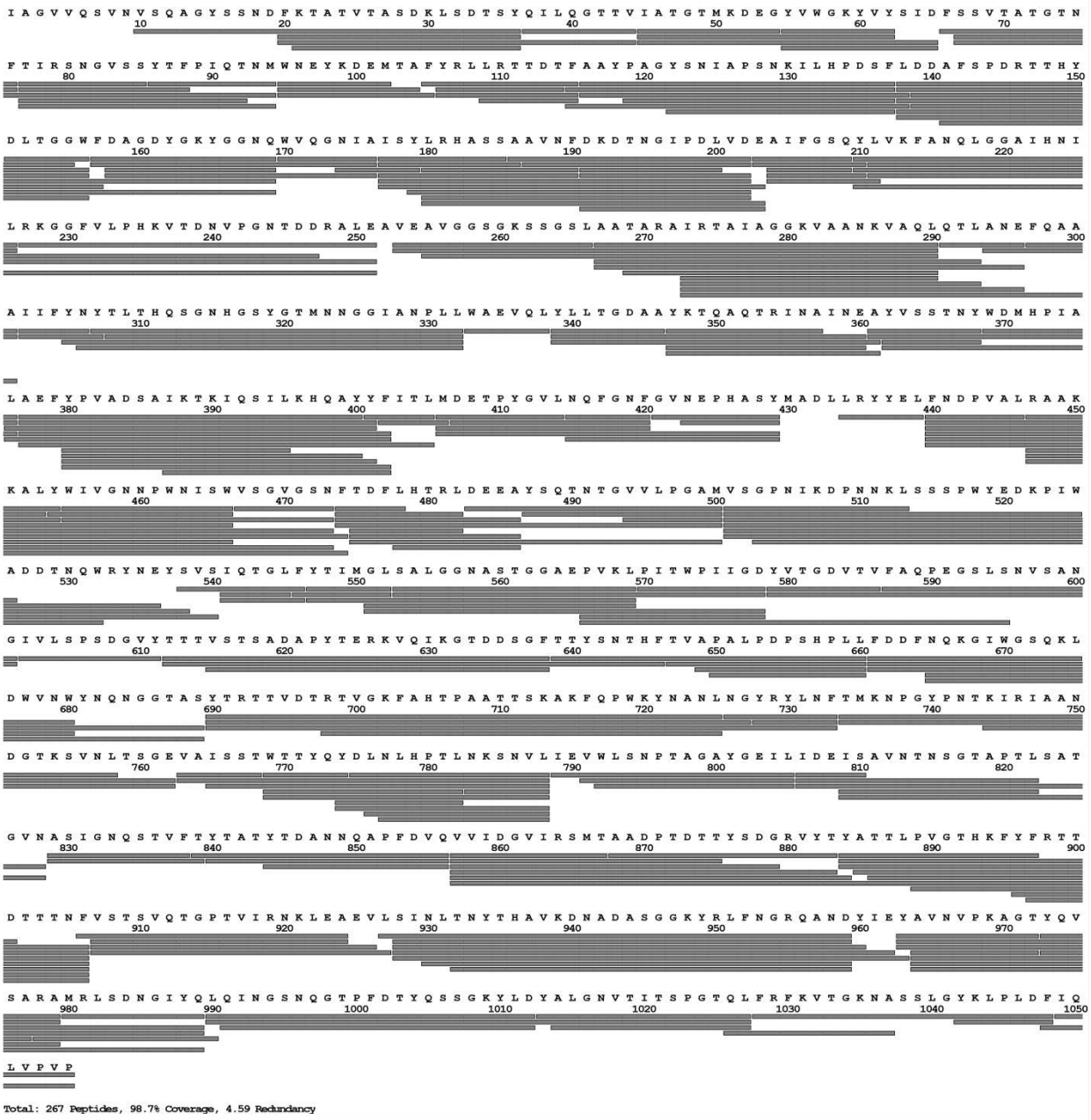

Figure S14 – Sequence coverage of *Psp*Xan9 in HDX-MS experiments. Peptic peptides identified by tandem MS which yielded MS signals of suitable quality to report on HDX are indicated by grey bars.

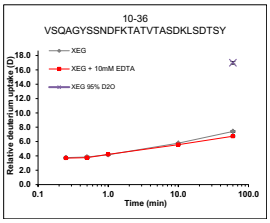
10-36
VSQAGYSSNDFKTATVTASDKLSDTSY
XEG
XEG + 10mM EDTA
XEG 95% D2O
Relative deuterium uptake (D)
Time (min)

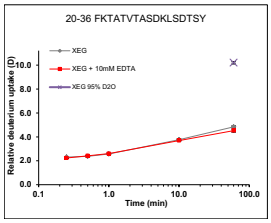
20-36 FKTATVTASDKLSDTSY
XEG
XEG + 10mM EDTA
XEG 95% D2O
Relative deuterium uptake (D)
Time (min)

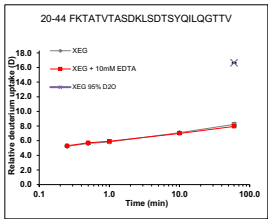
20-44 FKTATVTASDKLSDTSYQILQGTTV
XEG
XEG + 10mM EDTA
XEG 95% D2O
Relative deuterium uptake (D)
Time (min)

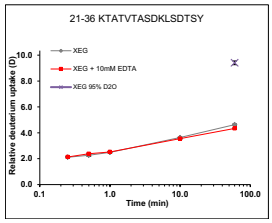
21-36 KTATVTASDKLSDTSY
XEG
XEG + 10mM EDTA
XEG 95% D2O
Relative deuterium uptake (D)
Time (min)

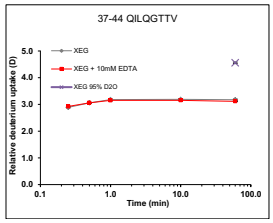
37-44 QILQGTTV
XEG
XEG + 10mM EDTA
XEG 95% D2O
Relative deuterium uptake (D)
Time (min)

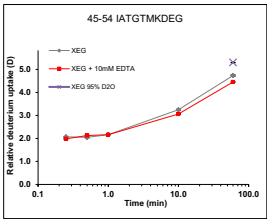
45-54 IATGTMKDEG
XEG
XEG + 10mM EDTA
XEG 95% D2O
Relative deuterium uptake (D)
Time (min)

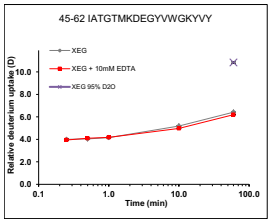
45-62 IATGTMKDEGYVWGKYVY
XEG
XEG + 10mM EDTA
XEG 95% D2O
Relative deuterium uptake (D)
Time (min)

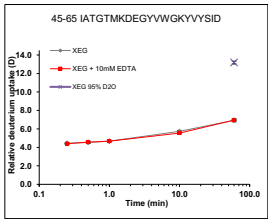
45-65 IATGTMKDEGYVWGKYVYSID
XEG
XEG + 10mM EDTA
XEG 95% D2O
Relative deuterium uptake (D)
Time (min)

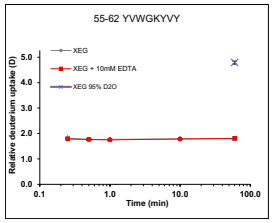
55-62 YVWGKYVY
XEG
XEG + 10mM EDTA
XEG 95% D2O
Relative deuterium uptake (D)
Time (min)

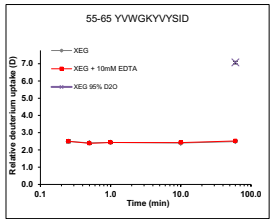
55-65 YVWGKYVYSID
XEG
XEG + 10mM EDTA
XEG 95% D2O
Relative deuterium uptake (D)
Time (min)

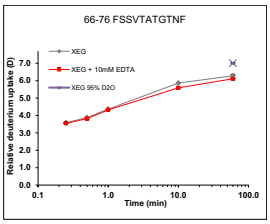
66-76 FSSVTATGTNF
XEG
XEG + 10mM EDTA
XEG 95% D2O
Relative deuterium uptake (D)
Time (min)

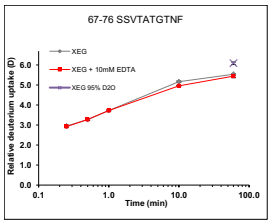
67-76 SSVTATGTNF
XEG
XEG + 10mM EDTA
XEG 95% D2O
Relative deuterium uptake (D)
Time (min)

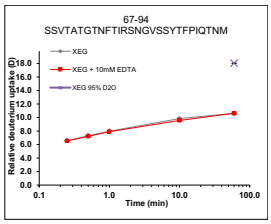
67-94
SSVTATGTNFTIRSNGVSSYTFPIQTNM
XEG
XEG + 10mM EDTA
XEG 95% D2O
Relative deuterium uptake (D)
Time (min)

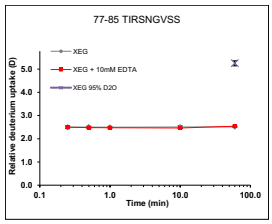
77-85 TIRSNGVSS
XEG
XEG + 10mM EDTA
XEG 95% D2O
Relative deuterium uptake (D)
Time (min)

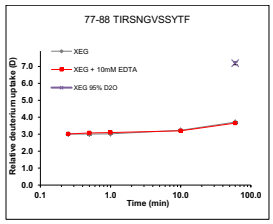
77-88 TIRSNGVSSYTF
XEG
XEG + 10mM EDTA
XEG 95% D2O
Relative deuterium uptake (D)
Time (min)

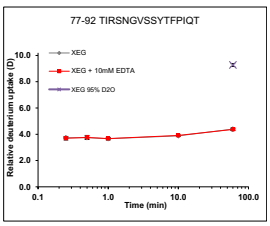
77-92 TIRSNGVSSYTFPIQT
XEG
XEG + 10mM EDTA
XEG 95% D2O
Relative deuterium uptake (D)
Time (min)

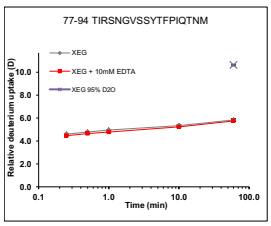
77-94 TIRSNGVSSYTFPIQTNM
XEG
XEG + 10mM EDTA
XEG 95% D2O
Relative deuterium uptake (D)
Time (min)

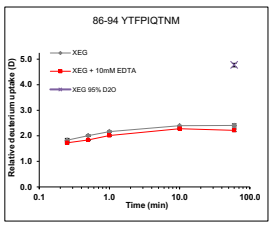
86-94 YTFPIQTNM
XEG
XEG + 10mM EDTA
XEG 95% D2O
Relative deuterium uptake (D)
Time (min)

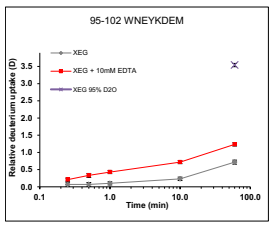
95-102 WNEYKDEM
XEG
XEG + 10mM EDTA
XEG 95% D2O
Relative deuterium uptake (D)
Time (min)

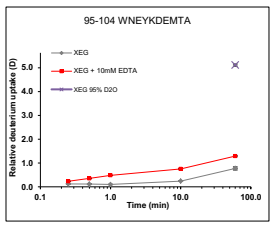
95-104 WNEYKDEMTA
XEG
XEG + 10mM EDTA
XEG 95% D2O
Relative deuterium uptake (D)
Time (min)

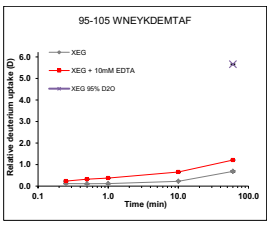
95-105 WNEYKDEMTAF
XEG
XEG + 10mM EDTA
XEG 95% D2O
Relative deuterium uptake (D)
Time (min)

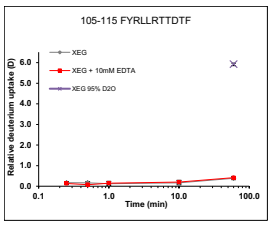
105-115 FYRLLRTTDTF
XEG
XEG + 10mM EDTA
XEG 95% D2O
Relative deuterium uptake (D)
Time (min)

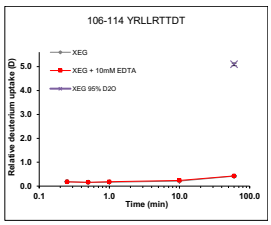
106-114 YRLLRTTDT
XEG
XEG + 10mM EDTA
XEG 95% D2O
Relative deuterium uptake (D)
Time (min)

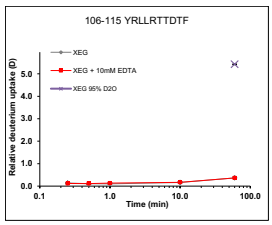
106-115 YRLLRTTDTF
XEG
XEG + 10mM EDTA
XEG 95% D2O
Relative deuterium uptake (D)
Time (min)

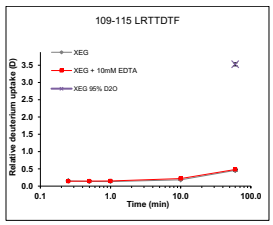
109-115 LRTTDTF
XEG
XEG + 10mM EDTA
XEG 95% D2O
Relative deuterium uptake (D)
Time (min)

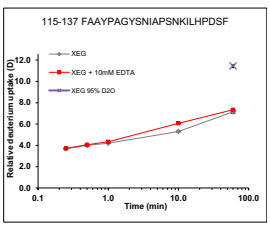
115-137 FAAYPAGYSNIAPSNKILHPDSF
XEG
XEG + 10mM EDTA
XEG 95% D2O
Relative deuterium uptake (D)
Time (min)

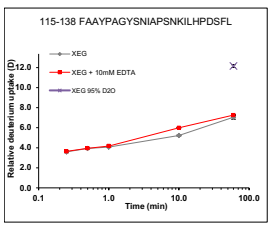
115-138 FAAYPAGYSNIAPSNKILHPDSFL
XEG
XEG + 10mM EDTA
XEG 95% D2O
Relative deuterium uptake (D)
Time (min)

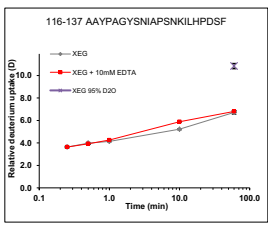
116-137 AAYPAGYSNIAPSNKILHPDSF
XEG
XEG + 10mM EDTA
XEG 95% D2O
Relative deuterium uptake (D)
Time (min)

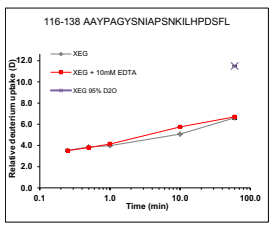
116-138 AAYPAGYSNIAPSNKILHPDSFL
XEG
XEG + 10mM EDTA
XEG 95% D2O
Relative deuterium uptake (D)
Time (min)

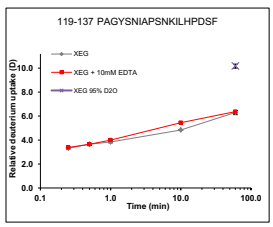
119-137 PAGYSNIAPSNKILHPDSF
XEG
XEG + 10mM EDTA
XEG 95% D2O
Relative deuterium uptake (D)
Time (min)

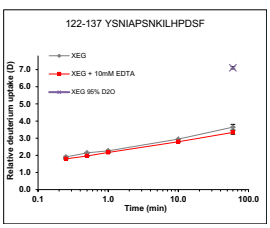
122-137 YSNIAPSNKILHPDSF
XEG
XEG + 10mM EDTA
XEG 95% D2O
Relative deuterium uptake (D)
Time (min)

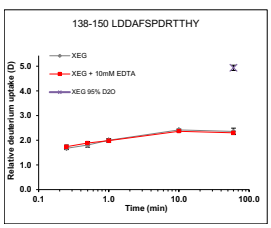
138-150 LDDAFSPDRTTHY
XEG
XEG + 10mM EDTA
XEG 95% D2O
Relative deuterium uptake (D)
Time (min)

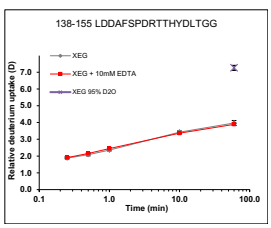
138-155 LDDAFSPDRTTHYDLTGG
XEG
XEG + 10mM EDTA
XEG 95% D2O
Relative deuterium uptake (D)
Time (min)

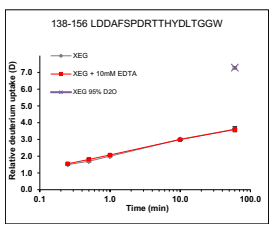
138-156 LDDAFSPDRTTHYDLTGGW
XEG
XEG + 10mM EDTA
XEG 95% D2O
Relative deuterium uptake (D)
Time (min)

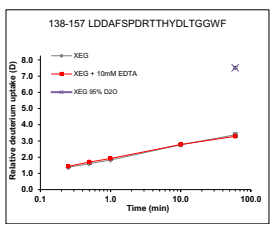
138-157 LDDAFSPDRTTHYDLTGGWF
XEG
XEG + 10mM EDTA
XEG 95% D2O
Relative deuterium uptake (D)
Time (min)

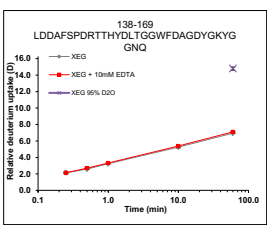
138-169
LDDAFSPDRTTHYDLTGGWFDAGDYGKYG
GNQ
XEG
XEG + 10mM EDTA
XEG 95% D2O
Relative deuterium uptake (D)
Time (min)

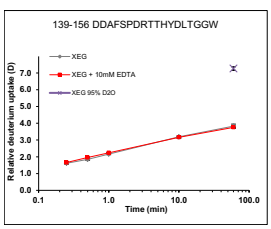
139-156 DDAFSPDRTTHYDLTGGW
XEG
XEG + 10mM EDTA
XEG 95% D2O
Relative deuterium uptake (D)
Time (min)

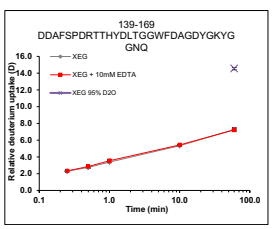
139-169
DDAFSPDRTTHYDLTGGWFDAGDYGKYG
GNQ
XEG
XEG + 10mM EDTA
XEG 95% D2O
Relative deuterium uptake (D)
Time (min)

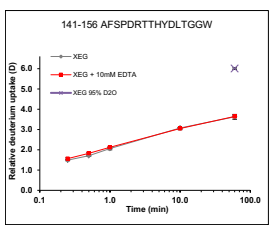
141-156 AFSPDRTTHYDLTGGW
XEG
XEG + 10mM EDTA
XEG 95% D2O
Relative deuterium uptake (D)
Time (min)

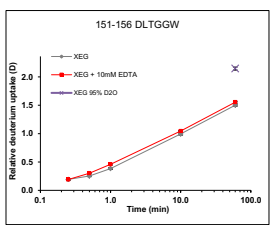
151-156 DLTGGW
XEG
XEG + 10mM EDTA
XEG 95% D2O
Relative deuterium uptake (D)
Time (min)

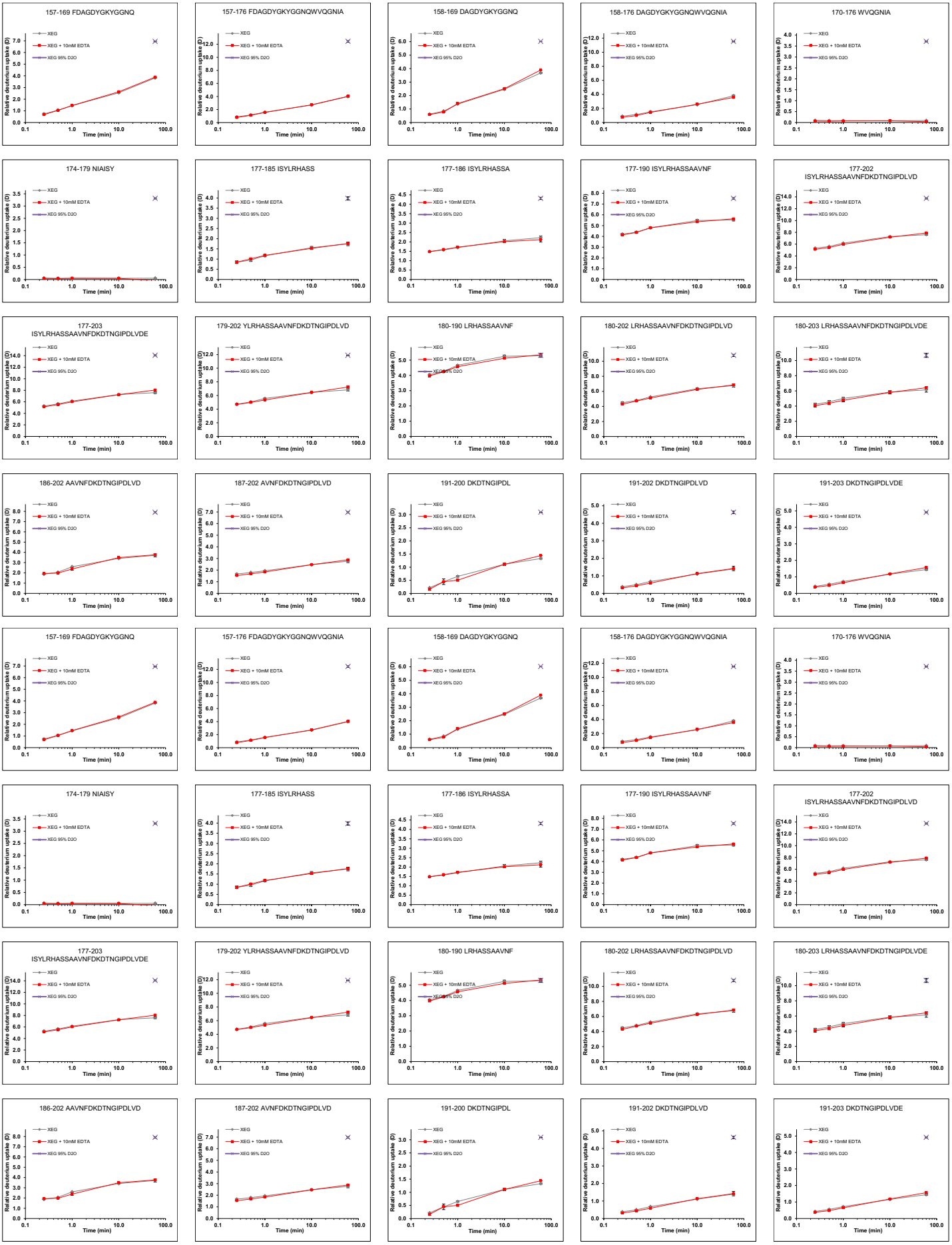
157-169 FDAGDYGKYGGNQ
157-176 FDAGDYGKYGGNQWVQGNIA
158-169 DAGDYGKYGGNQ
158-176 DAGDYGKYGGNQWVQGNIA
170-176 WVQGNIA
174-179 NIAISY
177-185 ISYLRHASS
177-186 ISYLRHASSA
177-190 ISYLRHASSAAVNF
177-202 ISYLRHASSAAVNFDKDTNGIPDLVD
177-203 ISYLRHASSAAVNFDKDTNGIPDLVDE
179-202 YLRHASSAAVNFDKDTNGIPDLVD
180-190 LRHASSAAVNF
180-202 LRHASSAAVNFDKDTNGIPDLVD
180-203 LRHASSAAVNFDKDTNGIPDLVDE
186-202 AAVNFDKDTNGIPDLVD
187-202 AVNFDKDTNGIPDLVD
191-200 DKDTNGIPDL
191-202 DKDTNGIPDLVD
191-203 DKDTNGIPDLVDE
XEG
XEG + 10mM EDTA
XEG 95% D2O
Relative deuterium uptake (D)
Time (min)

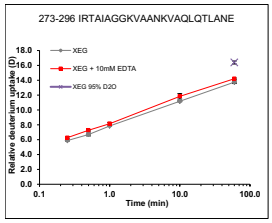
273-296 IRTAIAGGKVAANKVAQLQTLANE
XEG
XEG + 10mM EDTA
XEG 95% D2O
Relative deuterium uptake (D)
Time (min)

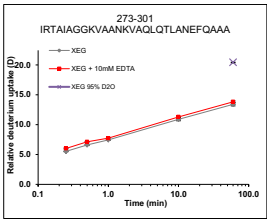
273-301
IRTAIAGGKVAANKVAQLQTLANEFQAAA
XEG
XEG + 10mM EDTA
XEG 95% D2O
Relative deuterium uptake (D)
Time (min)

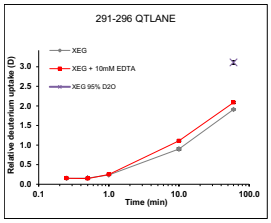
291-296 QTLANE
XEG
XEG + 10mM EDTA
XEG 95% D2O
Relative deuterium uptake (D)
Time (min)

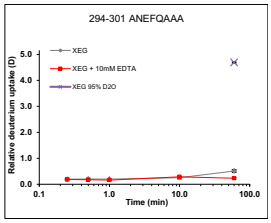
294-301 ANEFQAAA
XEG
XEG + 10mM EDTA
XEG 95% D2O
Relative deuterium uptake (D)
Time (min)

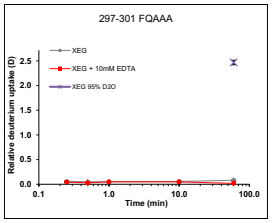
297-301 FQAAA
XEG
XEG + 10mM EDTA
XEG 95% D2O
Relative deuterium uptake (D)
Time (min)

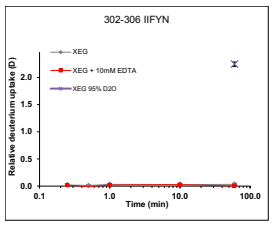
302-306 IIFYN
XEG
XEG + 10mM EDTA
XEG 95% D2O
Relative deuterium uptake (D)
Time (min)

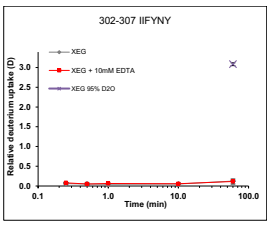
302-307 IIFYNY
XEG
XEG + 10mM EDTA
XEG 95% D2O
Relative deuterium uptake (D)
Time (min)

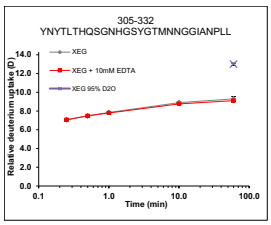
305-332
YNYTLTHQSGNHGSYGTMNNGGIANPLL
XEG
XEG + 10mM EDTA
XEG 95% D2O
Relative deuterium uptake (D)
Time (min)

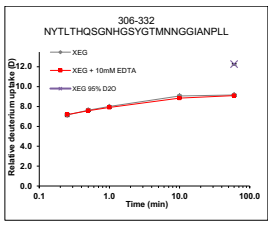
306-332
NYTLTHQSGNHGSYGTMNNGGIANPLL
XEG
XEG + 10mM EDTA
XEG 95% D2O
Relative deuterium uptake (D)
Time (min)

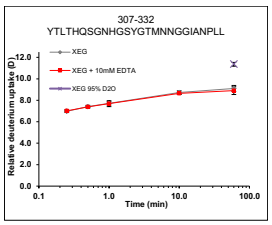
307-332
YTLTHQSGNHGSYGTMNNGGIANPLL
XEG
XEG + 10mM EDTA
XEG 95% D2O
Relative deuterium uptake (D)
Time (min)

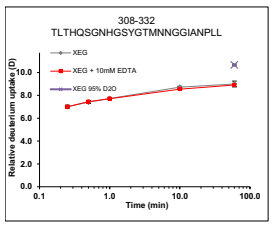
308-332
TLTHQSGNHGSYGTMNNGGIANPLL
XEG
XEG + 10mM EDTA
XEG 95% D2O
Relative deuterium uptake (D)
Time (min)

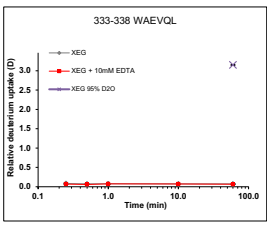
333-338 WAEVQL
XEG
XEG + 10mM EDTA
XEG 95% D2O
Relative deuterium uptake (D)
Time (min)

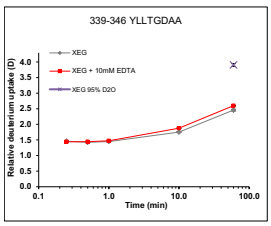
339-346 YLLTGDAA
XEG
XEG + 10mM EDTA
XEG 95% D2O
Relative deuterium uptake (D)
Time (min)

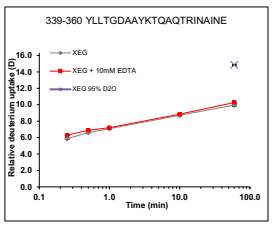
339-360 YLLTGDAAYKTQAQTRINAINE
XEG
XEG + 10mM EDTA
XEG 95% D2O
Relative deuterium uptake (D)
Time (min)

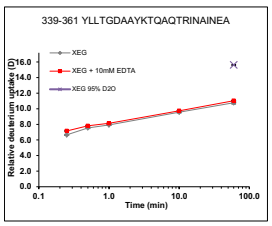
339-361 YLLTGDAAYKTQAQTRINAINEA
XEG
XEG + 10mM EDTA
XEG 95% D2O
Relative deuterium uptake (D)
Time (min)

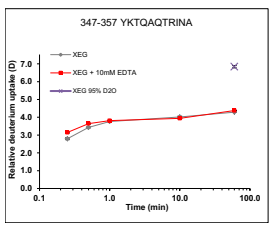
347-357 YKTQAQTRINA
XEG
XEG + 10mM EDTA
XEG 95% D2O
Relative deuterium uptake (D)
Time (min)

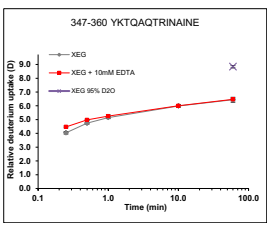
347-360 YKTQAQTRINAINE
XEG
XEG + 10mM EDTA
XEG 95% D2O
Relative deuterium uptake (D)
Time (min)

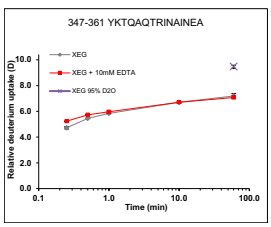
347-361 YKTQAQTRINAINEA
XEG
XEG + 10mM EDTA
XEG 95% D2O
Relative deuterium uptake (D)
Time (min)

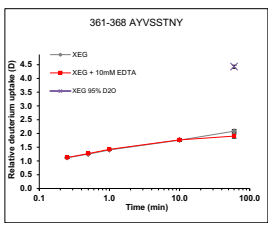
361-368 AYVSSTNY
XEG
XEG + 10mM EDTA
XEG 95% D2O
Relative deuterium uptake (D)
Time (min)

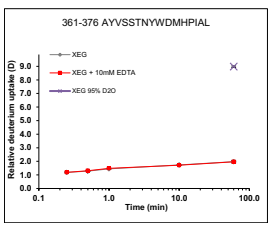
361-376 AYVSSTNYWDMHPIAL
XEG
XEG + 10mM EDTA
XEG 95% D2O
Relative deuterium uptake (D)
Time (min)

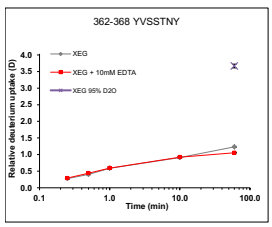
362-368 YVSSTNY
XEG
XEG + 10mM EDTA
XEG 95% D2O
Relative deuterium uptake (D)
Time (min)

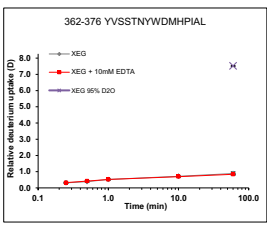
362-376 YVSSTNYWDMHPIAL
XEG
XEG + 10mM EDTA
XEG 95% D2O
Relative deuterium uptake (D)
Time (min)

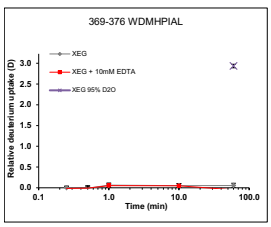
369-376 WDMHPIAL
XEG
XEG + 10mM EDTA
XEG 95% D2O
Relative deuterium uptake (D)
Time (min)

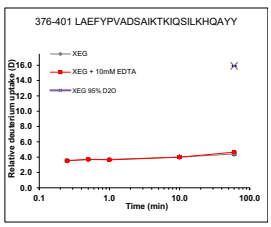
376-401 LAEFYPVADSAIKTKIQSILKHQAYY
XEG
XEG + 10mM EDTA
XEG 95% D2O
Relative deuterium uptake (D)
Time (min)

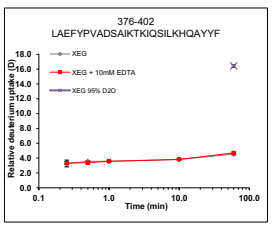
376-402
LAEFYPVADSAIKTKIQSILKHQAYYF
XEG
XEG + 10mM EDTA
XEG 95% D2O
Relative deuterium uptake (D)
Time (min)

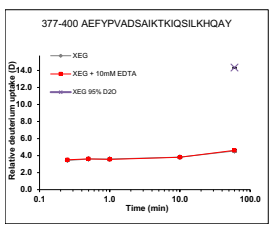
377-400 AEFYPVADSAIKTKIQSILKHQAY
XEG
XEG + 10mM EDTA
XEG 95% D2O
Relative deuterium uptake (D)
Time (min)

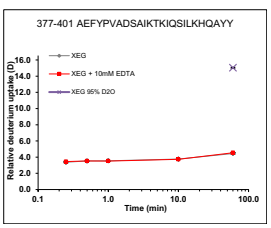
377-401 AEFYPVADSAIKTKIQSILKHQAYY
XEG
XEG + 10mM EDTA
XEG 95% D2O
Relative deuterium uptake (D)
Time (min)

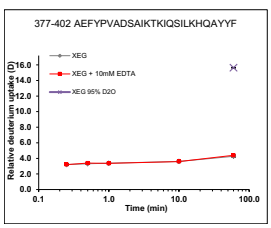
377-402 AEFYPVADSAIKTKIQSILKHQAYYF
XEG
XEG + 10mM EDTA
XEG 95% D2O
Relative deuterium uptake (D)
Time (min)

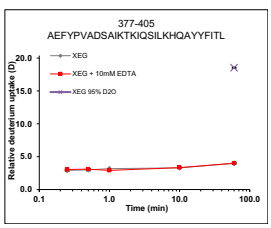
377-405
AEFYPVADSAIKTKIQSILKHQAYYFITL
XEG
XEG + 10mM EDTA
XEG 95% D2O
Relative deuterium uptake (D)
Time (min)

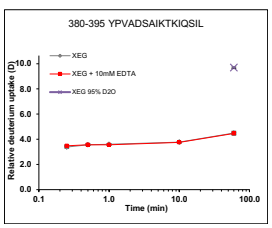
380-395 YPVADSAIKTKIQSIL
XEG
XEG + 10mM EDTA
XEG 95% D2O
Relative deuterium uptake (D)
Time (min)

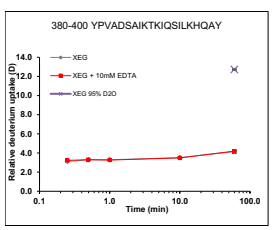
380-400 YPVADSAIKTKIQSILKHQAY
XEG
XEG + 10mM EDTA
XEG 95% D2O
Relative deuterium uptake (D)
Time (min)

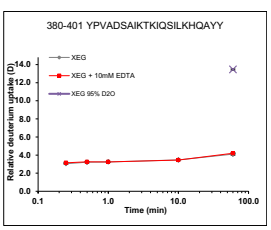
380-401 YPVADSAIKTKIQSILKHQAYY
XEG
XEG + 10mM EDTA
XEG 95% D2O
Relative deuterium uptake (D)
Time (min)

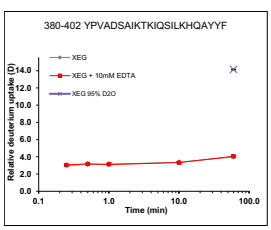
380-402 YPVADSAIKTKIQSILKHQAYYF
XEG
XEG + 10mM EDTA
XEG 95% D2O
Relative deuterium uptake (D)
Time (min)

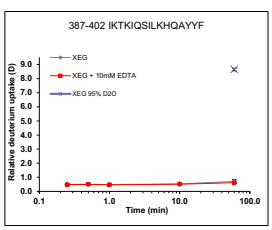
387-402 IKTKIQSILKHQAYYF
XEG
XEG + 10mM EDTA
XEG 95% D2O
Relative deuterium uptake (D)
Time (min)

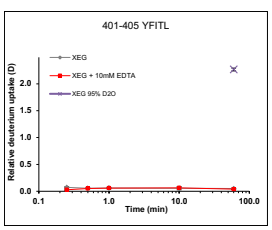
401-405 YFITL
XEG
XEG + 10mM EDTA
XEG 95% D2O
Relative deuterium uptake (D)
Time (min)

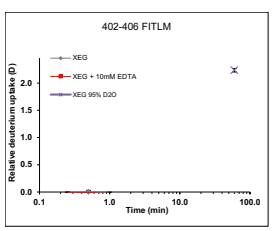
402-406 FITLM
XEG
XEG + 10mM EDTA
XEG 95% D2O
Relative deuterium uptake (D)
Time (min)

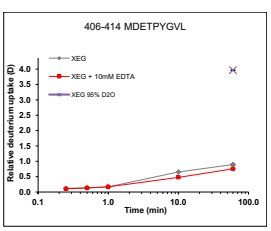
406-414 MDETPYGVL
XEG
XEG + 10mM EDTA
XEG 95% D2O
Relative deuterium uptake (D)
Time (min)

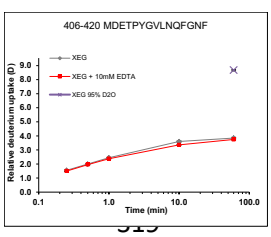
406-420 MDETPYGVLNQFGNF
XEG
XEG + 10mM EDTA
XEG 95% D2O
Relative deuterium uptake (D)
Time (min)

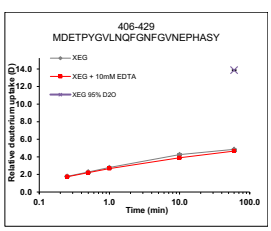
406-429
MDETPYGVLNQFGNFGVNEPHASY
XEG
XEG + 10mM EDTA
XEG 95% D2O
Relative deuterium uptake (D)
Time (min)

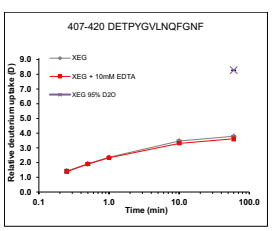
407-420 DETPYGVLNQFGNF
XEG
XEG + 10mM EDTA
XEG 95% D2O
Relative deuterium uptake (D)
Time (min)

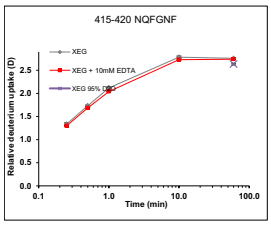
415-420 NQFGNF
XEG
XEG + 10mM EDTA
XEG 95% D2O
Relative deuterium uptake (D)
Time (min)

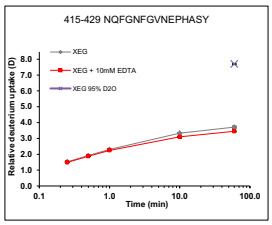
415-429 NQFGNFGVNEPHASY
XEG
XEG + 10mM EDTA
XEG 95% D2O
Relative deuterium uptake (D)
Time (min)

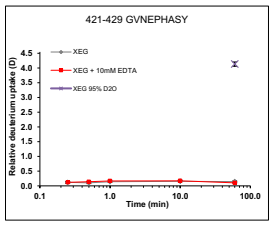
421-429 GVNEPHASY
XEG
XEG + 10mM EDTA
XEG 95% D2O
Relative deuterium uptake (D)
Time (min)

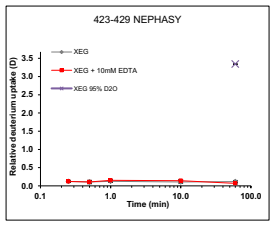
423-429 NEPHASY
XEG
XEG + 10mM EDTA
XEG 95% D2O
Relative deuterium uptake (D)
Time (min)

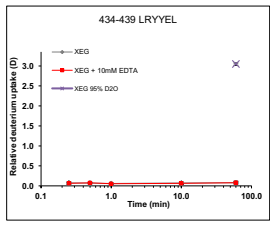
434-439 LRYYEL
XEG
XEG + 10mM EDTA
XEG 95% D2O
Relative deuterium uptake (D)
Time (min)

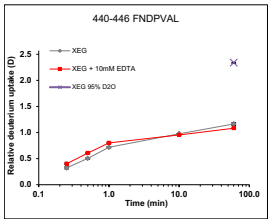
440-446 FNDPVAL
XEG
XEG + 10mM EDTA
XEG 95% D2O
Relative deuterium uptake (D)
Time (min)

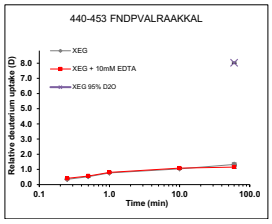
440-453 FNDPVALRAAKKAL
XEG
XEG + 10mM EDTA
XEG 95% D2O
Relative deuterium uptake (D)
Time (min)

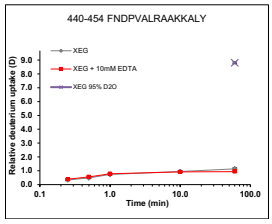
440-454 FNDPVALRAAKKALY
XEG
XEG + 10mM EDTA
XEG 95% D2O
Relative deuterium uptake (D)
Time (min)

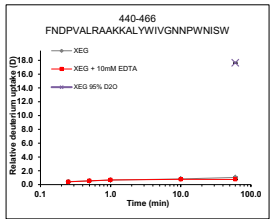
440-466
FNDPVALRAAKKALYWIVGNNPWNISW
XEG
XEG + 10mM EDTA
XEG 95% D2O
Relative deuterium uptake (D)
Time (min)

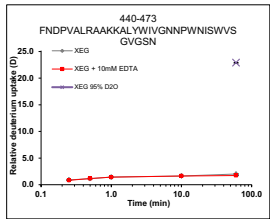
440-473
FNDPVALRAAKKALYWIVGNNPWNISWVS
GVGSN
XEG
XEG + 10mM EDTA
XEG 95% D2O
Relative deuterium uptake (D)
Time (min)

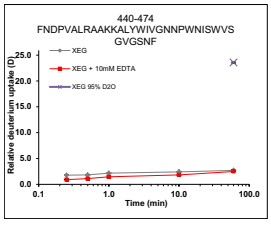
440-474
FNDPVALRAAKKALYWIVGNNPWNISWVS
GVGSNF
XEG
XEG + 10mM EDTA
XEG 95% D2O
Relative deuterium uptake (D)
Time (min)

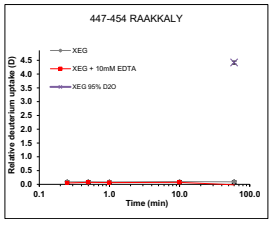
447-454 RAAKKALY
XEG
XEG + 10mM EDTA
XEG 95% D2O
Relative deuterium uptake (D)
Time (min)

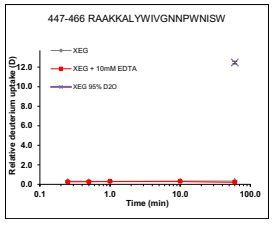
447-466 RAAKKALYWIVGNNPWNISW
XEG
XEG + 10mM EDTA
XEG 95% D2O
Relative deuterium uptake (D)
Time (min)

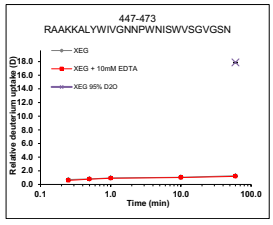
447-473
RAAKKALYWIVGNNPWNISWVSGVGSN
XEG
XEG + 10mM EDTA
XEG 95% D2O
Relative deuterium uptake (D)
Time (min)

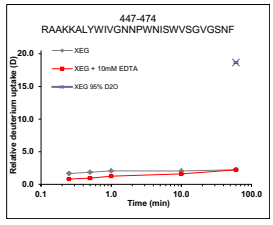
447-474
RAAKKALYWIVGNNPWNISWVSGVGSNF
XEG
XEG + 10mM EDTA
XEG 95% D2O
Relative deuterium uptake (D)
Time (min)

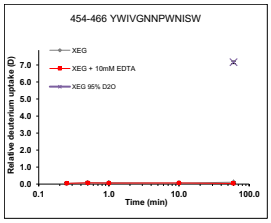
454-466 YWIVGNNPWNISW
XEG
XEG + 10mM EDTA
XEG 95% D2O
Relative deuterium uptake (D)
Time (min)

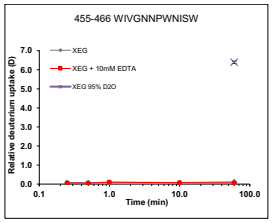
455-466 WIVGNNPWNISW
XEG
XEG + 10mM EDTA
XEG 95% D2O
Relative deuterium uptake (D)
Time (min)

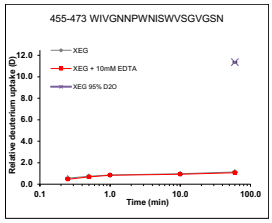
455-473 WIVGNNPWNISWVSGVGSN
XEG
XEG + 10mM EDTA
XEG 95% D2O
Relative deuterium uptake (D)
Time (min)

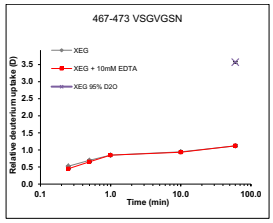
467-473 VSGVGSN
XEG
XEG + 10mM EDTA
XEG 95% D2O
Relative deuterium uptake (D)
Time (min)

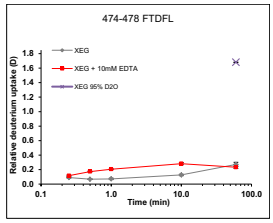
474-478 FTDFL
XEG
XEG + 10mM EDTA
XEG 95% D2O
Relative deuterium uptake (D)
Time (min)

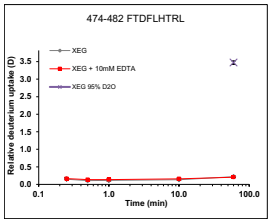
474-482 FTDFLHTRL
XEG
XEG + 10mM EDTA
XEG 95% D2O
Relative deuterium uptake (D)
Time (min)

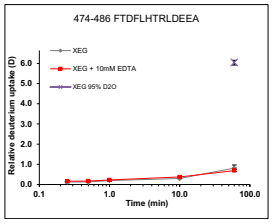
474-486 FTDFLHTRLDEEA
XEG
XEG + 10mM EDTA
XEG 95% D2O
Relative deuterium uptake (D)
Time (min)

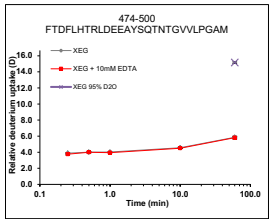
474-500
FTDFLHTRLDEEAYSQTNTGVVLPGAM
XEG
XEG + 10mM EDTA
XEG 95% D2O
Relative deuterium uptake (D)
Time (min)

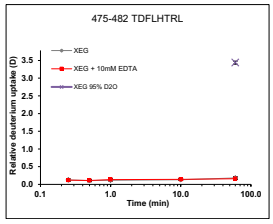
475-482 TDFLHTRL
XEG
XEG + 10mM EDTA
XEG 95% D2O
Relative deuterium uptake (D)
Time (min)

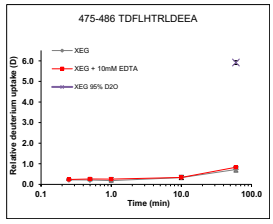
475-486 TDFLHTRLDEEA
XEG
XEG + 10mM EDTA
XEG 95% D2O
Relative deuterium uptake (D)
Time (min)

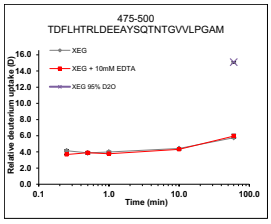
475-500
TDFLHTRLDEEAYSQTNTGVVLPGAM
XEG
XEG + 10mM EDTA
XEG 95% D2O
Relative deuterium uptake (D)
Time (min)

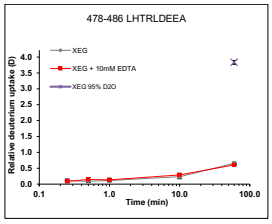
478-486 LHTRLDEEA
XEG
XEG + 10mM EDTA
XEG 95% D2O
Relative deuterium uptake (D)
Time (min)

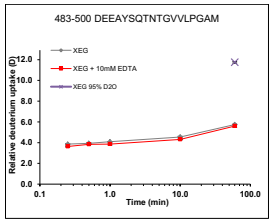
483-500 DEEAYSQTNTGVVLPGAM
XEG
XEG + 10mM EDTA
XEG 95% D2O
Relative deuterium uptake (D)
Time (min)

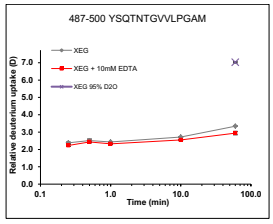
487-500 YSQTNTGVVLPGAM
XEG
XEG + 10mM EDTA
XEG 95% D2O
Relative deuterium uptake (D)
Time (min)

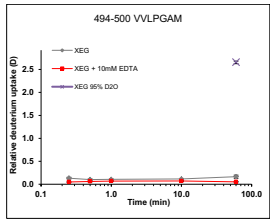
494-500 VVLPGAM
XEG
XEG + 10mM EDTA
XEG 95% D2O
Relative deuterium uptake (D)
Time (min)

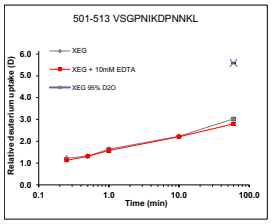
501-513 VSGPNIKDPNNKL
XEG
XEG + 10mM EDTA
XEG 95% D2O
Relative deuterium uptake (D)
Time (min)

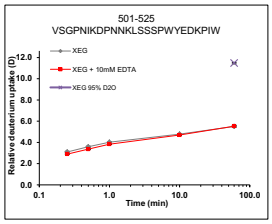
501-525
VSGPNIKDPNNKLSSSPWYEDKPIW
XEG
XEG + 10mM EDTA
XEG 95% D2O
Relative deuterium uptake (D)
Time (min)

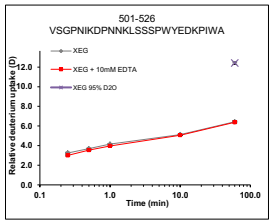
501-526
VSGPNIKDPNNKLSSSPWYEDKPIWA
XEG
XEG + 10mM EDTA
XEG 95% D2O
Relative deuterium uptake (D)
Time (min)

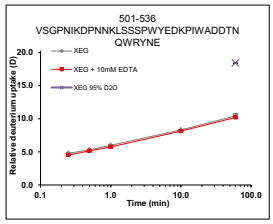
501-536
VSGPNIKDPNNKLSSSPWYEDKPIWADDTN
QWRYNE
XEG
XEG + 10mM EDTA
XEG 95% D2O
Relative deuterium uptake (D)
Time (min)

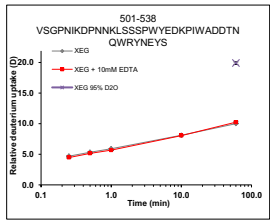
501-538
VSGPNIKDPNNKLSSSPWYEDKPIWADDTN
QWRYNEYS
XEG
XEG + 10mM EDTA
XEG 95% D2O
Relative deuterium uptake (D)
Time (min)

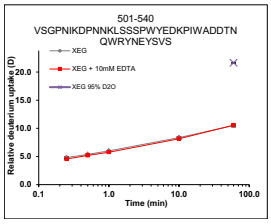
501-540
VSGPNIKDPNNKLSSSPWYEDKPIWADDTN
QWRYNEYSVS
XEG
XEG + 10mM EDTA
XEG 95% D2O
Relative deuterium uptake (D)
Time (min)

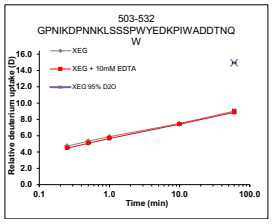
503-532
GPNIKDPNNKLSSSPWYEDKPIWADDTNQ
W
XEG
XEG + 10mM EDTA
XEG 95% D2O
Relative deuterium uptake (D)
Time (min)

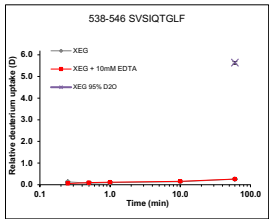
538-546 SVSIQTGLF
XEG
XEG + 10mM EDTA
XEG 95% D2O
Relative deuterium uptake (D)
Time (min)

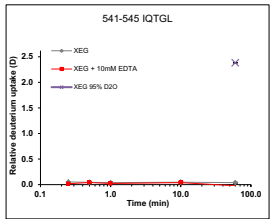
541-545 IQTGL
XEG
XEG + 10mM EDTA
XEG 95% D2O
Relative deuterium uptake (D)
Time (min)

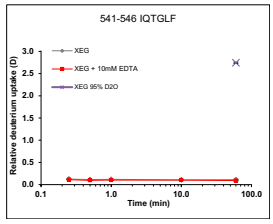
541-546 IQTGLF
XEG
XEG + 10mM EDTA
XEG 95% D2O
Relative deuterium uptake (D)
Time (min)

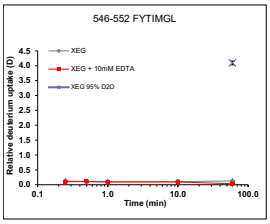
546-552 FYTIMGL
XEG
XEG + 10mM EDTA
XEG 95% D2O
Relative deuterium uptake (D)
Time (min)

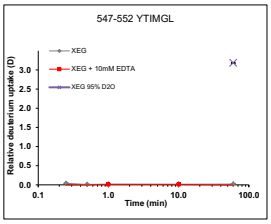
547-552 YTIMGL
XEG
XEG + 10mM EDTA
XEG 95% D2O
Relative deuterium uptake (D)
Time (min)

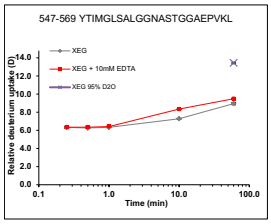
547-569 YTIMGLSALGGNASTGGAEPVKL
XEG
XEG + 10mM EDTA
XEG 95% D2O
Relative deuterium uptake (D)
Time (min)

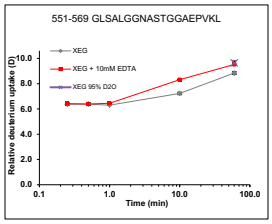
551-569 GLSALGGNASTGGAEPVKL
XEG
XEG + 10mM EDTA
XEG 95% D2O
Relative deuterium uptake (D)
Time (min)

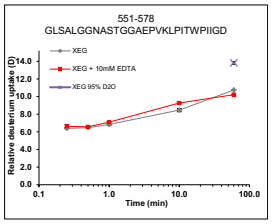
551-578
GLSALGGNASTGGAEPVKLPITWPIIGD
XEG
XEG + 10mM EDTA
XEG 95% D2O
Relative deuterium uptake (D)
Time (min)

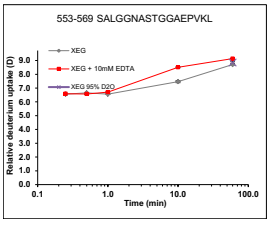
553-569 SALGGNASTGGAEPVKL
XEG
XEG + 10mM EDTA
XEG 95% D2O
Relative deuterium uptake (D)
Time (min)

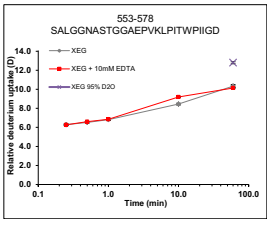
553-578
SALGGNASTGGAEPVKLPITWPIIGD
XEG
XEG + 10mM EDTA
XEG 95% D2O
Relative deuterium uptake (D)
Time (min)

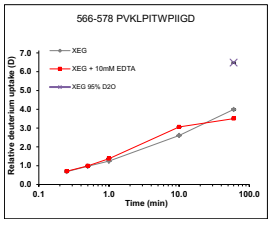
566-578 PVKLPITWPIIGD
XEG
XEG + 10mM EDTA
XEG 95% D2O
Relative deuterium uptake (D)
Time (min)

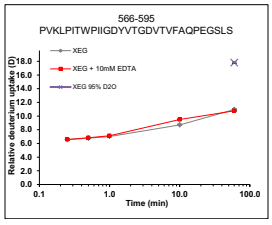
566-595
PVKLPITWPIIGDYVTGDVTVFAQPEGSLS
XEG
XEG + 10mM EDTA
XEG 95% D2O
Relative deuterium uptake (D)
Time (min)

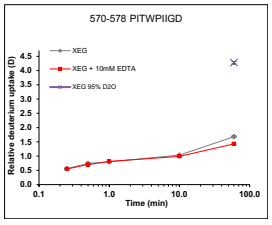
570-578 PITWPIIGD
XEG
XEG + 10mM EDTA
XEG 95% D2O
Relative deuterium uptake (D)
Time (min)

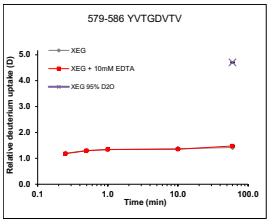
579-586 YVTGDVTV
XEG
XEG + 10mM EDTA
XEG 95% D2O
Relative deuterium uptake (D)
Time (min)

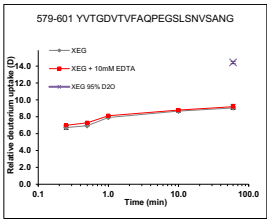
579-601 YVTGDVTVFAQPEGSLSNVSANG
XEG
XEG + 10mM EDTA
XEG 95% D2O
Relative deuterium uptake (D)
Time (min)

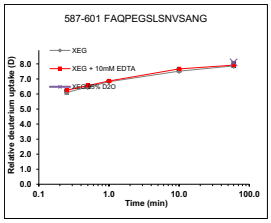
587-601 FAQPEGSLSNVSANG
XEG
XEG + 10mM EDTA
XEG 95% D2O
Relative deuterium uptake (D)
Time (min)

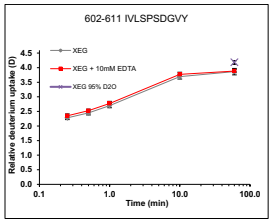
602-611 IVLSPSDGVY
XEG
XEG + 10mM EDTA
XEG 95% D2O
Relative deuterium uptake (D)
Time (min)

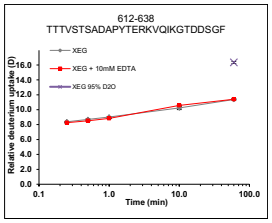
612-638
TTTVSTSADAPYTERKVQIKGTDDSGF
XEG
XEG + 10mM EDTA
XEG 95% D2O
Relative deuterium uptake (D)
Time (min)

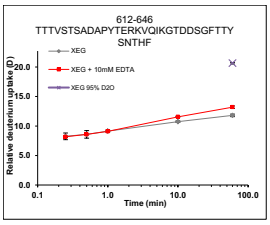
612-646
TTTVSTSADAPYTERKVQIKGTDDSGFTTY
SNTHF
XEG
XEG + 10mM EDTA
XEG 95% D2O
Relative deuterium uptake (D)
Time (min)

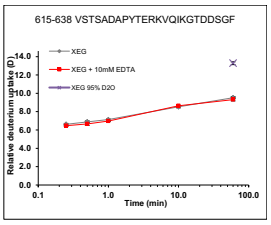
615-638 VSTSADAPYTERKVQIKGTDDSGF
XEG
XEG + 10mM EDTA
XEG 95% D2O
Relative deuterium uptake (D)
Time (min)

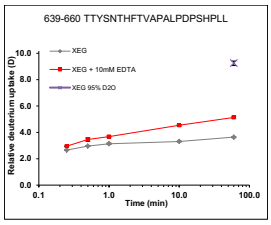
639-660 TTYSNTHFTVAPALPDPSHPLL
XEG
XEG + 10mM EDTA
XEG 95% D2O
Relative deuterium uptake (D)
Time (min)

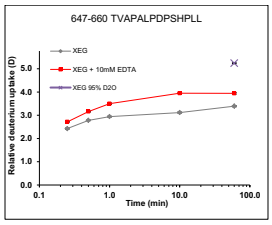
647-660 TVAPALPDPSHPLL
XEG
XEG + 10mM EDTA
XEG 95% D2O
Relative deuterium uptake (D)
Time (min)

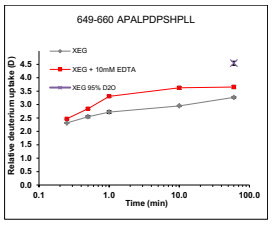
649-660 APALPDPSHPLL
XEG
XEG + 10mM EDTA
XEG 95% D2O
Relative deuterium uptake (D)
Time (min)

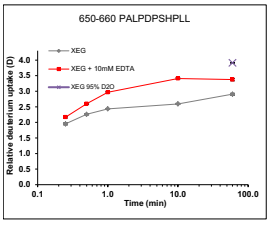
650-660 PALPDPSHPLL
XEG
XEG + 10mM EDTA
XEG 95% D2O
Relative deuterium uptake (D)
Time (min)

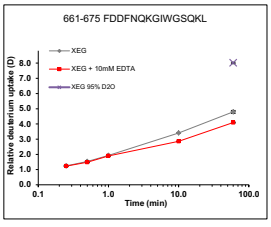
661-675 FDDFNQKGIWGSQKL
XEG
XEG + 10mM EDTA
XEG 95% D2O
Relative deuterium uptake (D)
Time (min)

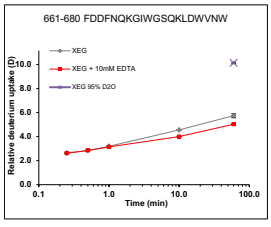
661-680 FDDFNQKGIWGSQKLDWVNW
XEG
XEG + 10mM EDTA
XEG 95% D2O
Relative deuterium uptake (D)
Time (min)

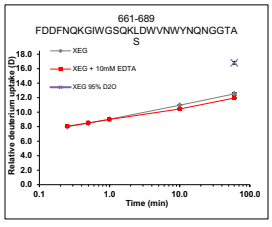
661-689
FDDFNQKGIWGSQKLDWVNWYNQNGGTA
S
XEG
XEG + 10mM EDTA
XEG 95% D2O
Relative deuterium uptake (D)
Time (min)

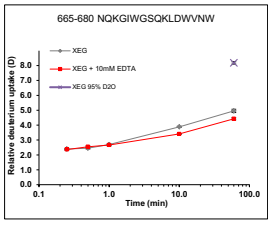
665-680 NQKGIWGSQKLDWVNW
XEG
XEG + 10mM EDTA
XEG 95% D2O
Relative deuterium uptake (D)
Time (min)

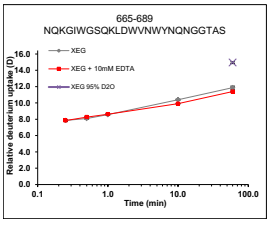
665-689
NQKGIWGSQKLDWVNWYNQNGGTAS
XEG
XEG + 10mM EDTA
XEG 95% D2O
Relative deuterium uptake (D)
Time (min)

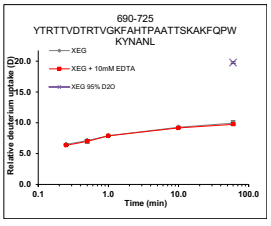
690-725
YTRTTVDTRTVGKFAHTPAATTSKAKFQPW
KYNANL
XEG
XEG + 10mM EDTA
XEG 95% D2O
Relative deuterium uptake (D)
Time (min)

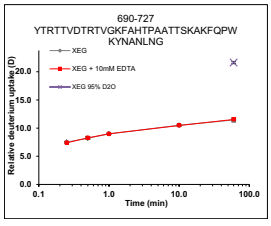
690-727
YTRTTVDTRTVGKFAHTPAATTSKAKFQPW
KYNANLNG
XEG
XEG + 10mM EDTA
XEG 95% D2O
Relative deuterium uptake (D)
Time (min)

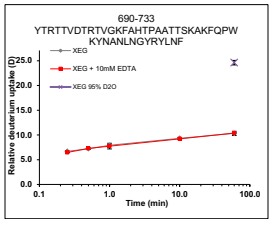
690-733
YTRTTVDTRTVGKFAHTPAATTSKAKFQPW
KYNANLNGYRYLNF
XEG
XEG + 10mM EDTA
XEG 95% D2O
Relative deuterium uptake (D)
Time (min)

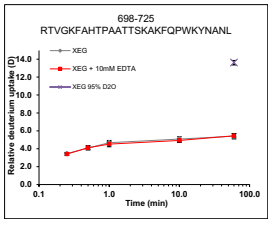
698-725
RTVGKFAHTPAATTSKAKFQPWKYNANL
XEG
XEG + 10mM EDTA
XEG 95% D2O
Relative deuterium uptake (D)
Time (min)

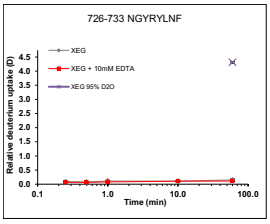
726-733 NGYRYLNF
XEG
XEG + 10mM EDTA
XEG 95% D2O
Relative deuterium uptake (D)
Time (min)

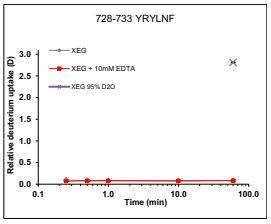
728-733 YRYLNF
XEG
XEG + 10mM EDTA
XEG 95% D2O
Relative deuterium uptake (D)
Time (min)

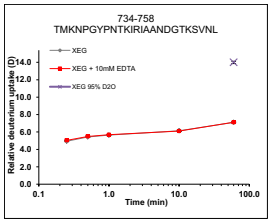
734-758
TMKNPGYPNTKIRIAANDGTKSVNL
XEG
XEG + 10mM EDTA
XEG 95% D2O
Relative deuterium uptake (D)
Time (min)

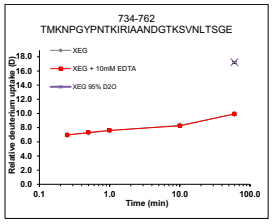
734-762
TMKNPGYPNTKIRIAANDGTKSVNLTSGE
XEG
XEG + 10mM EDTA
XEG 95% D2O
Relative deuterium uptake (D)
Time (min)

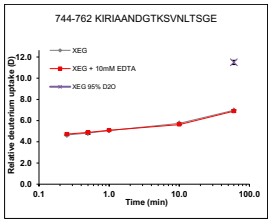
744-762 KIRIAANDGTKSVNLTSGE
XEG
XEG + 10mM EDTA
XEG 95% D2O
Relative deuterium uptake (D)
Time (min)

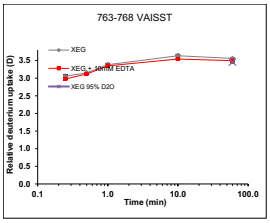
763-768 VAISST
XEG
XEG + 10mM EDTA
XEG 95% D2O
Relative deuterium uptake (D)
Time (min)

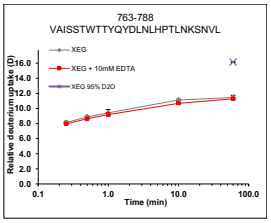
763-788
VAISSTWTTYQYDLNLHPTLNKSNVL
XEG
XEG + 10mM EDTA
XEG 95% D2O
Relative deuterium uptake (D)
Time (min)

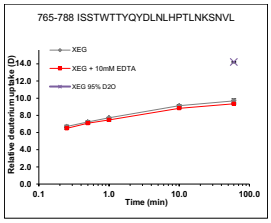
765-788 ISSTWTTYQYDLNLHPTLNKSNVL
XEG
XEG + 10mM EDTA
XEG 95% D2O
Relative deuterium uptake (D)
Time (min)

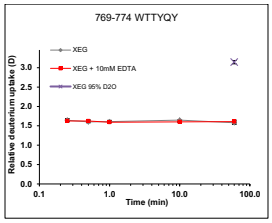
769-774 WTTYQY
XEG
XEG + 10mM EDTA
XEG 95% D2O
Relative deuterium uptake (D)
Time (min)

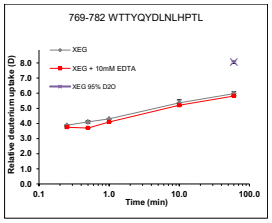
769-782 WTTYQYDLNLHPTL
XEG
XEG + 10mM EDTA
XEG 95% D2O
Relative deuterium uptake (D)
Time (min)

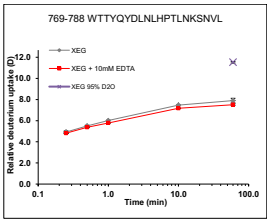
769-788 WTTYQYDLNLHPTLNKSNVL
XEG
XEG + 10mM EDTA
XEG 95% D2O
Relative deuterium uptake (D)
Time (min)

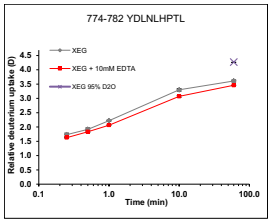
774-782 YDLNLHPTL
XEG
XEG + 10mM EDTA
XEG 95% D2O
Relative deuterium uptake (D)
Time (min)

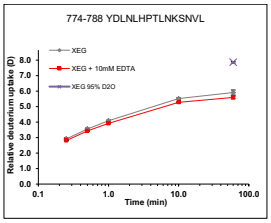
774-788 YDLNLHPTLNKSNVL
XEG
XEG + 10mM EDTA
XEG 95% D2O
Relative deuterium uptake (D)
Time (min)

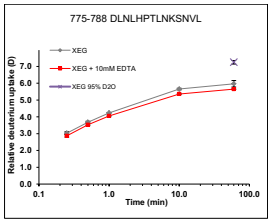
775-788 DLNLHPTLNKSNVL
XEG
XEG + 10mM EDTA
XEG 95% D2O
Relative deuterium uptake (D)
Time (min)

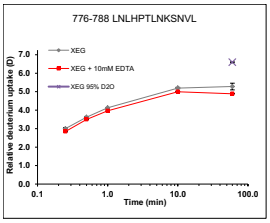
776-788 LNLHPTLNKSNVL
XEG
XEG + 10mM EDTA
XEG 95% D2O
Relative deuterium uptake (D)
Time (min)

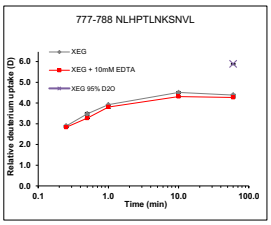
777-788 NLHPTLNKSNVL
XEG
XEG + 10mM EDTA
XEG 95% D2O
Relative deuterium uptake (D)
Time (min)

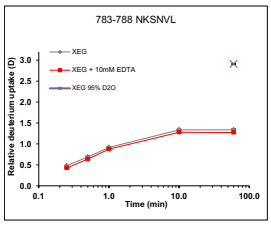
783-788 NKSNVL
XEG
XEG + 10mM EDTA
XEG 95% D2O
Relative deuterium uptake (D)
Time (min)

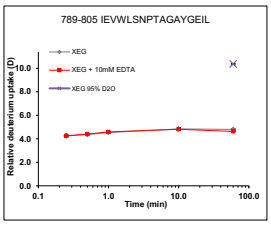
789-805 IEVWLSNPTAGAYGEIL
XEG
XEG + 10mM EDTA
XEG 95% D2O
Relative deuterium uptake (D)
Time (min)

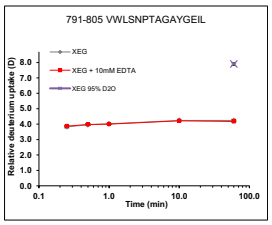
791-805 VWLSNPTAGAYGEIL
XEG
XEG + 10mM EDTA
XEG 95% D2O
Relative deuterium uptake (D)
Time (min)

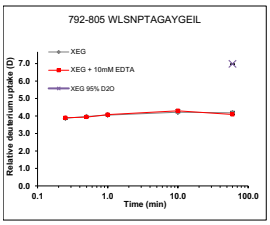
792-805 WLSNPTAGAYGEIL
XEG
XEG + 10mM EDTA
XEG 95% D2O
Relative deuterium uptake (D)
Time (min)

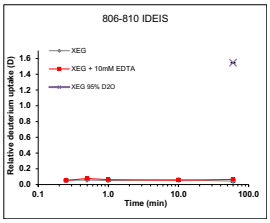
806-810 IDEIS
XEG
XEG + 10mM EDTA
XEG 95% D2O
Relative deuterium uptake (D)
Time (min)

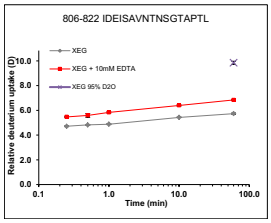
806-822 IDEISAVNTNSGTAPTL
XEG
XEG + 10mM EDTA
XEG 95% D2O
Relative deuterium uptake (D)
Time (min)

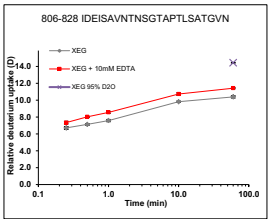
806-828 IDEISAVNTNSGTAPTLSATGVN
XEG
XEG + 10mM EDTA
XEG 95% D2O
Relative deuterium uptake (D)
Time (min)

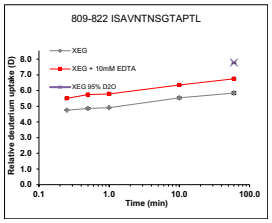
809-822 ISAVNTNSGTAPTL
XEG
XEG + 10mM EDTA
XEG 95% D2O
Relative deuterium uptake (D)
Time (min)

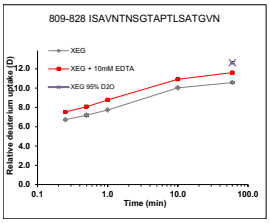
809-828 ISAVNTNSGTAPTLSATGVN
XEG
XEG + 10mM EDTA
XEG 95% D2O
Relative deuterium uptake (D)
Time (min)

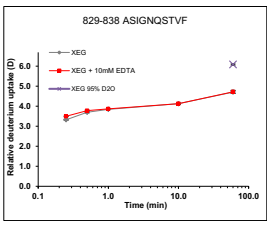
829-838 ASIGNQSTVF
XEG
XEG + 10mM EDTA
XEG 95% D2O
Relative deuterium uptake (D)
Time (min)

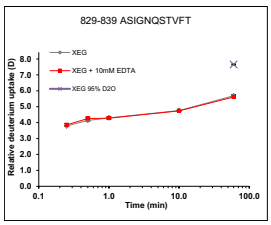
829-839 ASIGNQSTVFT
XEG
XEG + 10mM EDTA
XEG 95% D2O
Relative deuterium uptake (D)
Time (min)

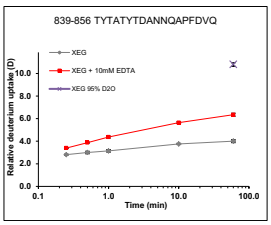
839-856 TYTATYTDANNQAPFDVQ
XEG
XEG + 10mM EDTA
XEG 95% D2O
Relative deuterium uptake (D)
Time (min)

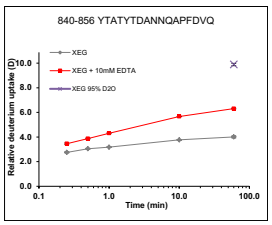
840-856 YTATYTDANNQAPFDVQ
XEG
XEG + 10mM EDTA
XEG 95% D2O
Relative deuterium uptake (D)
Time (min)

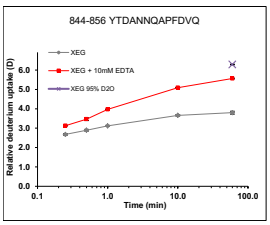
844-856 YTDANNQAPFDVQ
XEG
XEG + 10mM EDTA
XEG 95% D2O
Relative deuterium uptake (D)
Time (min)

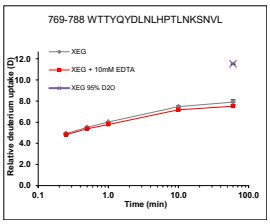
769-788 WTTYQYDLNLHPTLNKSNVL
XEG
XEG + 10mM EDTA
XEG 95% D2O
Relative deuterium uptake (D)
Time (min)

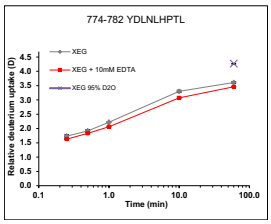
774-782 YDLNLHPTL
XEG
XEG + 10mM EDTA
XEG 95% D2O
Relative deuterium uptake (D)
Time (min)

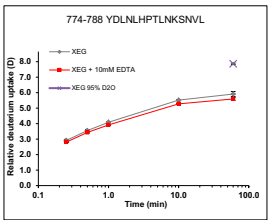
774-788 YDLNLHPTLNKSNVL
XEG
XEG + 10mM EDTA
XEG 95% D2O
Relative deuterium uptake (D)
Time (min)

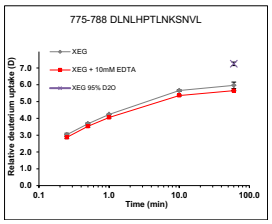
775-788 DLNLHPTLNKSNVL
XEG
XEG + 10mM EDTA
XEG 95% D2O
Relative deuterium uptake (D)
Time (min)

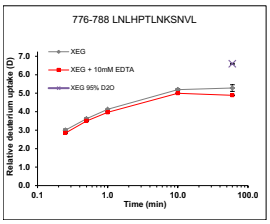
776-788 LNLHPTLNKSNVL
XEG
XEG + 10mM EDTA
XEG 95% D2O
Relative deuterium uptake (D)
Time (min)

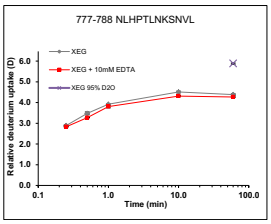
777-788 NLHPTLNKSNVL
XEG
XEG + 10mM EDTA
XEG 95% D2O
Relative deuterium uptake (D)
Time (min)

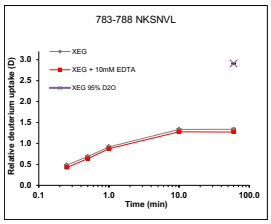
783-788 NKSNVL
XEG
XEG + 10mM EDTA
XEG 95% D2O
Relative deuterium uptake (D)
Time (min)

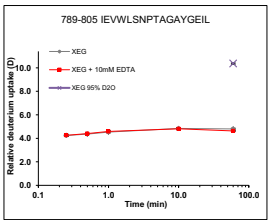
789-805 IEVWLSNPTAGAYGEIL
XEG
XEG + 10mM EDTA
XEG 95% D2O
Relative deuterium uptake (D)
Time (min)

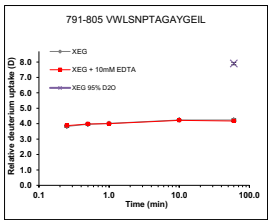
791-805 VWLSNPTAGAYGEIL
XEG
XEG + 10mM EDTA
XEG 95% D2O
Relative deuterium uptake (D)
Time (min)

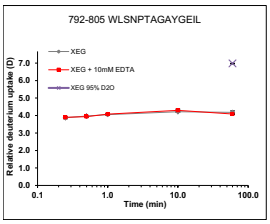
792-805 WLSNPTAGAYGEIL
XEG
XEG + 10mM EDTA
XEG 95% D2O
Relative deuterium uptake (D)
Time (min)

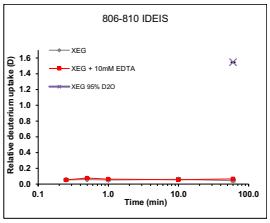
806-810 IDEIS
XEG
XEG + 10mM EDTA
XEG 95% D2O
Relative deuterium uptake (D)
Time (min)

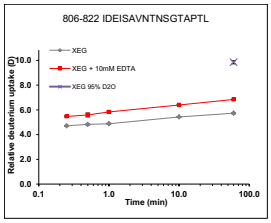
806-822 IDEISAVNTNSGTAPTL
XEG
XEG + 10mM EDTA
XEG 95% D2O
Relative deuterium uptake (D)
Time (min)

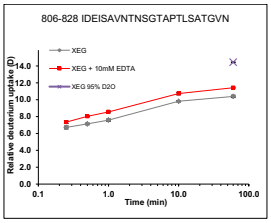
806-828 IDEISAVNTNSGTAPTLSATGVN
XEG
XEG + 10mM EDTA
XEG 95% D2O
Relative deuterium uptake (D)
Time (min)

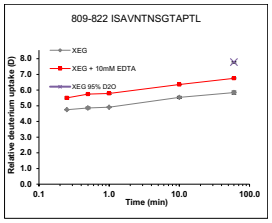
809-822 ISAVNTNSGTAPTL
XEG
XEG + 10mM EDTA
XEG 95% D2O
Relative deuterium uptake (D)
Time (min)

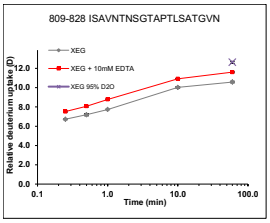
809-828 ISAVNTNSGTAPTLSATGVN
XEG
XEG + 10mM EDTA
XEG 95% D2O
Relative deuterium uptake (D)
Time (min)

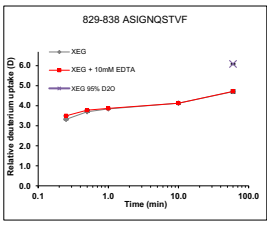
829-838 ASIGNQSTVF
XEG
XEG + 10mM EDTA
XEG 95% D2O
Relative deuterium uptake (D)
Time (min)

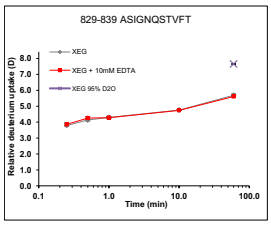
829-839 ASIGNQSTVFT
XEG
XEG + 10mM EDTA
XEG 95% D2O
Relative deuterium uptake (D)
Time (min)

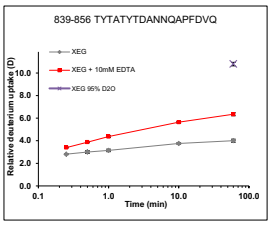
839-856 TYTATYTDANNQAPFDVQ
XEG
XEG + 10mM EDTA
XEG 95% D2O
Relative deuterium uptake (D)
Time (min)

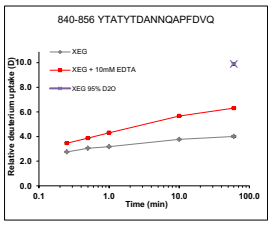
840-856 YTATYTDANNQAPFDVQ
XEG
XEG + 10mM EDTA
XEG 95% D2O
Relative deuterium uptake (D)
Time (min)

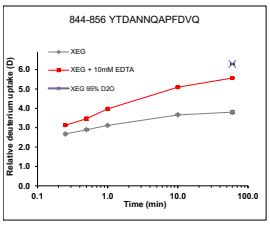
844-856 YTDANNQAPFDVQ
XEG
XEG + 10mM EDTA
XEG 95% D2O
Relative deuterium uptake (D)
Time (min)

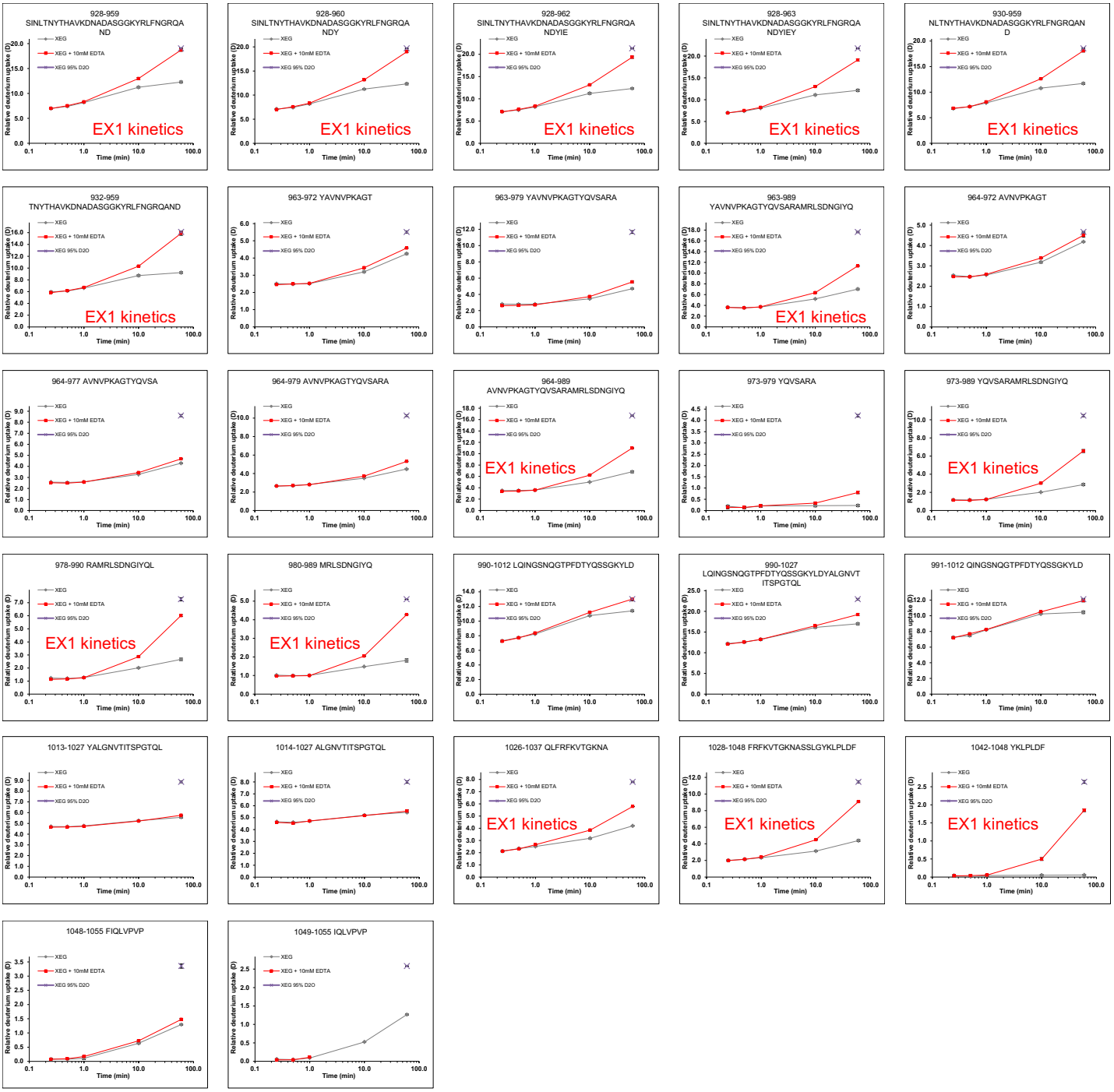

Figure S15 – Deuterium uptake plots of *Psp*Xan9. The deuterium incorporation of *Psp*Xan9 peptic peptides in the absence (grey) and presence of 10 mM EDTA (red) was determined in triplicate HDX-MS experiments at 15 s. 30 s, 1 min, 10 min and 1 h and plotted with 1 x standard deviation (black). The fully deuterated control (95% D_2O) is shown in purple at the last time point (1 h). Note: *Psp*Xan9 is labelled as XEG.

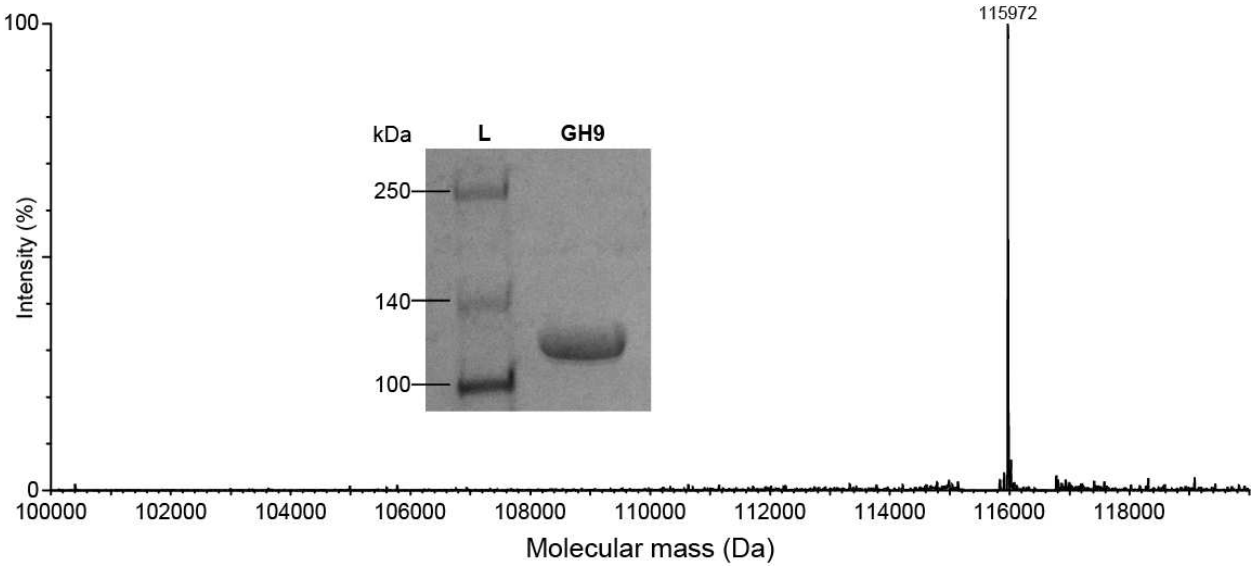

Figure S16 – Purity and molecular mass analysis of recombinant *Psp*Xan9. *Inset*: SDS-PAGE analysis of *Psp*Xan9 (lane 'GH9') versus a molecular weight ladder (lane 'L'). Intact-protein mass spectrometry indicates a single peak of mass 115972 versus 115969 calculated from the mature amino acid sequence.

TABLES

Table S1 – ^{1}H and ^{13}C assignments of the lyase-treated xanthan tetrasaccharide.

Monosaccharide ^{1}H	δ (ppm)	Multiplicity	Coupling constant (J) (Hz)	Monosaccharide ^{13}C	δ (ppm)
Glc(r) —				*Glc(r) —*	
α H1	5.20	d	3.74	*α C1*	92.13
β H1	4.64	d	7.76	*β C1*	96.13
α H2	3.59	m	n.a.	*α C2*	70.05
β H2	3.26	dd	8.71; 8.71	*β C2*	72.92
α H3	4.00	t	9.47	*α C3*	76.11
β H3	3.81	t	9.67	*β C3*	78.84
α/β H4	3.90	t	9.48	*α/β C4*	76.11
α H5	3.58	m	n.a.	*α C5*	70.05
β H5	3.56	ddd	n.a.	*β C5*	75.01
α H6	3.87; n.a.	m	n.a.	*α C6*	59.08
β H6	n.a.; n.a.	n.a.	n.a.	*β C6*	n.a.
Glc(n.r.) —				*Glc(n.r.) —*	
H1	4.44	d	7.59	*C1*	102.07
H2	3.20	dd	8.78; 17.5	*C2*	73.67
H3	3.47	t	9.25	*C3*	75.61
H4	3.05	m	n.a.	*C4*	70.86
H5	3.41	dd	9.34; 6.39	*C5*	77.07
H6/6'	3.54; 3.84	m; d	n.a.; 11.38	*C6*	61.66
Man —				*Man —*	
H1	5.35; 5.38	d; d	<1; <1	*C1*	98.96
H2	4.29	dd	n.a.	*C2*	77.67
H3	3.90	m	n.a.	*C3*	69.66
H4	3.79	t	10.35	*C4*	66.03
H5	4.05	m	n.a.	*C5*	72.40
H6/6'	n.a.; n.a.	n.a.	n.a.	*C6*	
Δ4,5-ene-GlcA —				*Δ4,5-ene-GlcA —*	
H1	4.82; 4.83	d; d	8.26; 8.26	*C1*	101.50
H2	3.63	dd	7.96; 7.96	*C2*	70.77
H3	4.34	dd	7.18; 2.80	*C3*	68.68
H4	5.74	d	2.26	*C4*	108.73
				C5	145.57
				C6	168.65

n.a. (not assigned) indicates that an unambiguous assignment was not possible due to overlapping peaks.

Table S2 – Data quality and structure refinement statistics

Data set	Native	Pt
PDB code	6FHJ	6FHN
Beamline	Diamond I04-1	Diamond I03
Wavelength (Å)	0.92	1.07
Space group	$P3_221$	$P3_221$
Cell parameters (Å)	a=103.35 b=103.35 c=212.5	a=103.27 b=103.27 c=210.35
Resolution range (Å)[a]	27.50-2.09 (2.09-2.04)	52.59-2.00 (2.05-2.00)
Number of reflections	858487	877195
Unique reflections	84289	88513
Monomers in asymmetric unit	1	1
Completeness %	99.9 (99.9)	100.0 (100.0)
I/I(σ)	15.8(3.6)	16.0 (3.5)
CC(1/2)[c]	0.999(0.878)	0.999 (0.876)
Average multiplicity	10.2 (10.5)	9.9 (9.8)
R_{merge} (%)[b]	9.9 (65.0)	8.2 (64.0)
Refinement statistics		
Percentage of R_{free} reflections	4.98	5.01
(%)R_{cryst}=Σ||Fo| - |Fc||/Σ|Fo|(%)	17.6	17.3
Free R factor (%)	20.3	20.8
Bond distances (Å):	0.013	0.012
Bond angles (°):	1.15	1.58
Average protein B values (Å^2)	34	39
Molprobity score	1.4	1.75
Ramachandran Plot [d]		
Most favoured	90.0	89.8
Additionally allowed	9.2	9.3
Generously allowed	0.6	0.5
Disallowed	0.2	0.4

[a] Values in parentheses correspond to the highest resolution shell.
[b] R_{merge} is defined as 100x Σ\|I - <I>\|/ Σ I, where I is the intensity of the reflection.
[c] CC(1/2) values for Imean are calculated by splitting the data randomly in half.
[d] Ramachandran plot analysis was carried out using PROCHECK[2].

Table S3 – Differential relative deuterium incorporation in percent of *Psp*Xan9 in the absence and presence of chelating agent. Increases and reductions in differential relative deuterium uptake are written in red and blue respectively

Domain	Region	15s	30s	1min	10min	60 min
X229	46-54	-	-	-	>-2.5%	> -5%
	68-76	-	-	-	>-2.5%	-
	87-94	-	>-2.5%	>-2.5%	-	-
GH9	95-105	>2.5%	>5%	>7.5%	> 10%	> 10%
	116-122	-	-	-	>5%	-
	152-156	-	-	>2.5%	-	-
	192-200	-	-	>-2.5%	-	> 2.5%
	228-251	-	-	-	-	> 5%
	274-290	-	>2.5%	>2.5%		
	292-296	-	-	-	>5%	> 5%
	297-301	-	-	-	-	> -2.5%
	340-346	-	-	-	>2.5%	> 2.5%
	348-357	>5% (348-361)	>2.5%	-	-	-
	362-368	-	-	-	-	> -5%
	370-376	-	-	-	-	> -2.5%
	406-414	-	-	-	> -2.5%	> -2.5%
	441-454	>2.5%	>2.5	>2.5%	-	> -2.5 %
	475-478	-	>5%	>7.5%	-	-
	488-513	-	-	-	-	>- 5%
	542-545	-	-	-	-	>-2.5%
β1	553-566	-	-	-	>10%	>5%
	567-570	-	-	-	>5%	> -7.5%
	571-578	-	-	-	-	> - 5%
	640-647	>2.5%	>5%	>5%	>12.5%	> 15%
	648-660	>5%	>7.5%	>12.5%	>20%	>10%
β2	662-680	-	-	-	>-5%	>-5%
	681-689	-	-	-	>-2.5%	>-2.5%
	775-781	-	-	>-2.5%	>-5%	>-2.5
β3	811-822	>7.5%	>10%	>10%	>10%	>10%
	823-828	>5%	>5%	>7.5%	>5%	> 5%
	841-844	>5%	>7.5%	>10%	>17.5%	>20%
	845-856	>5%	>7.5%	>12.5%	>22.5%	>25%
	869-883	>10%	>10%	>7.5%	-	>5%
	897-906	>5%	>12.5%	>20%	>55%	>55%
CBM84	907-924	-	-	-	>5%	>7.5%
	925-927	-	-	-	>10%	>15%
	928-959	-	-	-	**EX1**	**EX1**
	973-989	-	-	-	**EX1**	**EX1**
	991-1012	-	-	-	-	>10%
	1028-1048	-	-	-	**EX1**	**EX1**
	1049-1055	-	-	-	>5%	>5%

Table S4– Differential relative deuterium incorporation for selected regions (absolute values) of *Psp*Xan9 in the absence and presence of chelating agent. For the time-point where the most pronounced difference occurs the value is highlighted in red.

Peptide 95-105	Time (min)	0,25	0,5	1	10	60
	ΔHDX (*Psp*Xan9 EDTA-*Psp*Xan9) (Da)	0,11	0,21	0,26	0,43	0,52

Peptide 227-251	Time (min)	0,25	0,5	1	10	60
	ΔHDX (*Psp*Xan9 EDTA-*Psp*Xan9) (Da)	0,00	0,04	0,04	0,05	0,67

Peptide 291-296	Time (min)	0,25	0,5	1	10	60
	ΔHDX (*Psp*Xan9 EDTA-*Psp*Xan9) (Da)	0,01	-0,01	0,01	0,21	0,18

Peptide 551-569	Time (min)	0,25	0,5	1	10	60
	ΔHDX (*Psp*Xan9 EDTA-*Psp*Xan9) (Da)	0,05	0,00	0,15	1,08	0,68

Peptide 639-660	Time (min)	0,25	0,5	1	10	60
	ΔHDX (*Psp*Xan9 EDTA-*Psp*Xan9) (Da)	0,29	0,50	0,54	1,23	1,49

Peptide 809-822	Time (min)	0,25	0,5	1	10	60
	ΔHDX (*Psp*Xan9 EDTA-*Psp*Xan9) (Da)	0,75	0,88	0,88	0,82	0,91

Peptide 840-856	Time (min)	0,25	0,5	1	10	60
	ΔHDX (*Psp*Xan9 EDTA-*Psp*Xan9) (Da)	0,71	0,82	1,13	1,90	2,30

Peptide 897-906	Time (min)	0,25	0,5	1	10	60
	ΔHDX (*Psp*Xan9 EDTA-*Psp*Xan9) (Da)	0,36	0,70	1,11	2,95	2,97

Peptide 907-927	Time (min)	0,25	0,5	1	10	60
	ΔHDX (*Psp*Xan9 EDTA-*Psp*Xan9) (Da)	-0,04	0,08	0,20	1,47	2,66

Peptide 928-959	Time (min)	0,25	0,5	1	10	60
	ΔHDX (*Psp*Xan9 EDTA-*Psp*Xan9) (Da)	-0,03	0,13	0,15	1,75	6,42

Peptide 980-989	Time (min)	0,25	0,5	1	10	60
	ΔHDX (*Psp*Xan9 EDTA-*Psp*Xan9) (Da)	-0,05	-0,01	-0,01	0,56	2,46

Peptide 1028-1048	Time (min)	0,25	0,5	1	10	60
	ΔHDX (*Psp*Xan9 EDTA-*Psp*Xan9) (Da)	-0,01	-0,02	0,07	1,37	4,68

Table S5 - Composition of liquid model detergent used

Ingredient	Amount (g)
Sodium dodecylbenzenesulfonate	174.7
Sodium lauryl ether sulfate (28% in water)	1146.4
Soy fatty acid (based on C16-18 fatty acids)	30
BIO-SOFT N25-7 (alcohol ethoxylate with 7 moles ethoxylate; based on C12-15 alcohol)	159
Water	1400
Triethanolamine	12
Sodium hydroxide	15.7
Sodium citrate	60
Calcium chloride	0.6
Total	2998.4

REFERENCES

1. Domon, B.; Costello, C. E., A Systematic Nomenclature for Carbohydrate Fragmentations in Fab-Ms Ms Spectra of Glycoconjugates. *Glycoconjugate J.* **1988,** *5*, 397-409.
2. Laskowski, R. A.; Macarthur, M. W.; Moss, D. S.; Thornton, J. M., Procheck - a Program to Check the Stereochemical Quality of Protein Structures. *J. Appl. Crystallogr.* **1993,** *26*, 283-291.